Volume 6 JULY, 1935 Number 7

PHYSICS

A Journal of General and Applied Physics

Floating Grid Direct-Current Amplifier

P. A. MACDONALD AND E. M. CAMPBELL, *Winnipeg, Canada*

(Received March 30, 1935)

It is shown that commercial screen grid radio tubes are suitable for high sensitivity direct-current amplifiers. The theoretical limit due to the Johnson effect has been observed and agrees with the calculated value. Tubes when operated at floating grid are capable of detecting 2×10^{-16} ampere, the theoretical limit of the tube. Absolute linearity of response exists at least up to currents of 2×10^{-12} ampere.

THE current sensitivity of a single tube direct-current amplifier is given by

$$di_p/di = G_m/(1/R_g + 1/Z_g), \qquad (1)$$

where G_m is the mutual conductance of the tube, Z_g the reciprocal of the slope of the grid potential *vs.* grid current curve, which quantity has been defined as the grid impedance[1] and R_g the value of the input resistor, i being the input current and i_p the current in the plate circuit.

If an open circuit is used in place of the input resistor the control grid initially assumes a definite potential depending upon the constants of the circuit. This potential is termed floating grid potential. With such a circuit, Eq. (1) simplifies to

$$di_p/di = G_m Z_g. \qquad (2)$$

Provided suitable control can be exercised over the values of G_m and Z_g which are usually interdependent, the floating grid circuit will have an advantage over the resistor circuit when it is desired to approach the limiting current sensitivity of the tube, as Z_g determines this quantity. It is the purpose of this communication to point out that such a condition may be realized employing commercial screen grid radio tubes.

The operating constants of a screen grid tube used for direct-current amplification have been discussed at some length elsewhere[2] and it has been shown that when a grid resistor is employed the most suitable operating characteristics for the UX 222 are obtained with a plate potential less than that of the screen grid and with a potential of the screen grid in the vicinity of 12 volts, the filament voltage being kept as low as is consistent with steady electron emission.

Control of Floating Grid Potential

The first requisite for a successful floating grid circuit is to be able to place the floating grid potential at any desired point on the mutual conductance curve. It has been pointed out in the previous communication[2] that the mutual conductance curves are moved to regions of greater negative bias in direct proportion to an increase in the screen grid potential, the maximum value of the mutual conductance remaining unaltered.

The effect of the screen grid potential upon the potential of floating grid has been examined experimentally, the results being shown graphically in Figs. 1 and 2. It will be seen that the floating grid potential rises slightly with increasing screen grid potential, the relation being strictly linear. Hence latitude in the position of the floating grid potential relative to the mutual

[1] W. B. Nottingham, J. Frank. Inst. **209**, 287 (1930).

[2] P. A. Macdonald and T. W. Tweed, Physics **4**, 178 (1933).

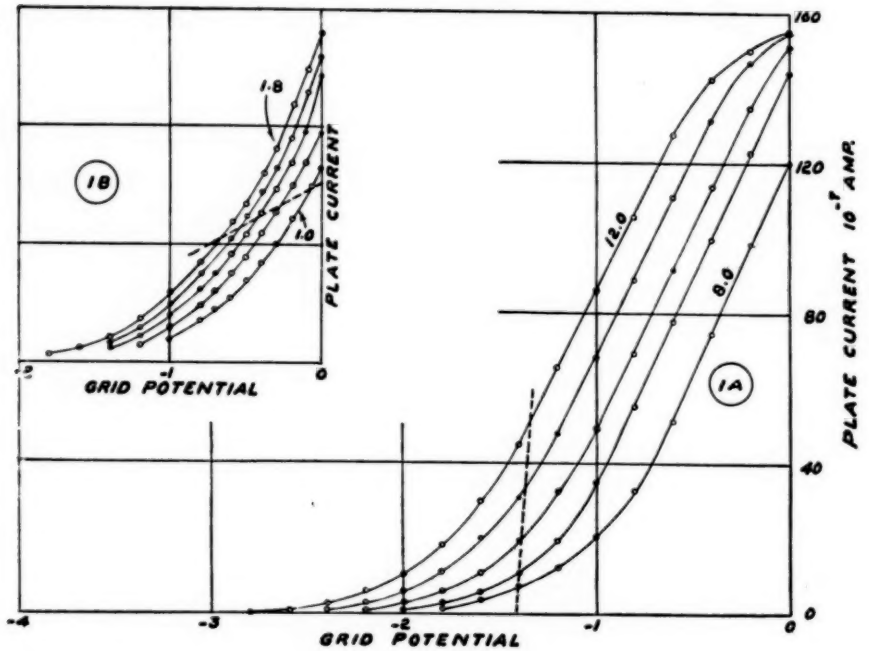

FIG. 1. The broken line across these curves represents the locus of floating grid potential. The group of curves on the right-hand side of the figure shows the manner in which the screen grid potential may be utilized to place the floating grid on the linear section of the grid potential *vs.* plate current curve. The family of curves marked 1*B* is obtained for different filament potentials, and shows that this potential may be used to accomplish the same purpose.

conductance curve is allowed by manipulation of the screen grid potential. Fig. 1A shows that such control is adequate; Fig. 1B shows that the filament voltage accomplishes the same purpose. However, control by the filament cannot in general be used practically as the value of Z_g decreases rapidly with increasing filament current.

GRID IMPEDANCE CHARACTERISTICS

A second requisite for a successful floating grid amplifier is the existence of a linear relation between the input current and the potential of the control grid.

In order to determine this range of constant grid impedance, grid potential *vs.* plate current curves were run with a high resistor of known value in series between the control grid potentiometer and this grid, the high resistor was then removed and the curves repeated. In the first instance the grid potential E_g is related to the applied potential V_g from the potentiometer in the grid circuit, by the equation

$$E_g = V_g - R_g i_g, \tag{3}$$

R_g being the value of the resistor employed and i_g the grid current. Differentiating this equation with respect to E_g gives

$$di_g/dE_g = (1/R_g)(dV_g/dE_g - 1), \tag{4}$$

which may be written

$$Z_g = R_g/[(dV_g/di_p)\cdot(di_p/dE_g) - 1]. \tag{5}$$

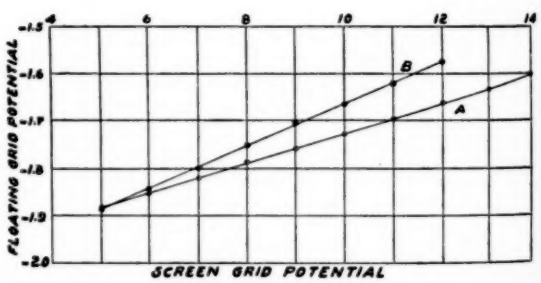

FIG. 2. Data obtained for two different filament voltages showing that the floating grid potential is directly proportional to the screen grid potential.

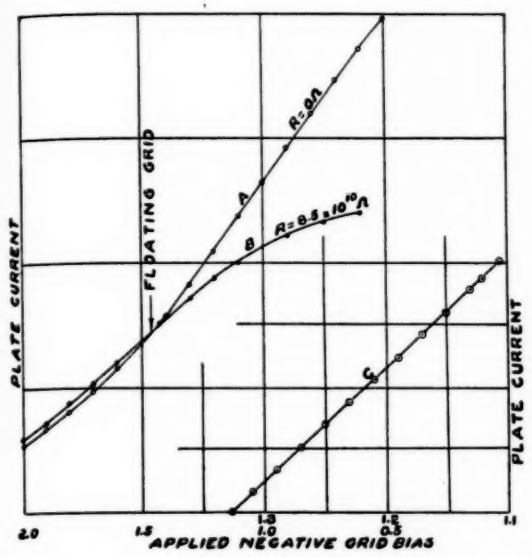

FIG. 3. Data showing the existence of a constant grid impedance in the vicinity of the floating grid potential. The grid impedance is constant over the grid potential range in which curves *A* and *B* are both straight. Curve *C* is another curve obtained in a manner similar to *B* but plotted on a larger scale to show more clearly the linear relation.

The numerical value of dV_g/di_p is obtained from the applied grid bias *vs.* plate current curve run with R_g in the circuit, di_p/dE_g being obtained from the corresponding curve obtained by omitting R_g. It is thus apparent that over the plate current range in which the ratio of these two slopes is constant the grid impedance is also constant.

Fig. 3 shows a set of data obtained in the above manner, the floating grid potential being designated by an arrow. Curves *A* and *B* show the data obtained without and with the resistor, respectively. Since these are straight over a range in excess of 0.2 volt starting at floating grid, the grid impedance is constant over this range. *C* is another curve run with a resistor in the grid circuit and plotted on a larger scale to demonstrate more clearly the existence of a linear relation. The numerical value of the grid impedance obtained from such curves averaged 10^{11} ohms for a number of different 222 tubes.

This datum thus shows that linear amplification will result for a grid potential rise of 0.2 volt across an impedance of 10^{11} ohms, that is, for the range of currents between 0 and 2×10^{-12} amp.

SMALLEST DETECTABLE CURRENT

The smallest current that may be detected is considered to be limited by the Schott and Johnson effects. Equations, enabling the numerical values anticipated by these effects to be calculated for direct-current amplifiers have been derived by L. R. Hafstad[3] from the original equations. He calculates a voltage fluctuation on the basis of the Johnson effect of $\pm3\times10^{-5}$ volt. For the Schott effect it is approximately $\pm10^{-4}$ volt.

In order to test these limits practically, a single tube amplifier was constructed with a 10,000-ohm resistor in the plate circuit across which was shunted a galvanometer and a back e.m.f. from an external dry cell to compensate for the plate current through the galvanometer. The tube was allowed to stand in a vacuum for twelve hours after which period an irregular fluctuation of $\pm2\times10^{-5}$ volt/division, observed after the first hour, was still present, superimposed upon a drift of six divisions a minute. These observations were repeated with a number of tubes of the same type and it was found that approximately three out of twelve would give similar results, the remainder gave large irregular fluctuations and showed much larger drifts. It was accordingly concluded that approximately 25 percent of the commercial screen grid tubes were suitable for use in such a circuit and that the limit of sensitivity set by the Schott and Johnson effects had been observed. It will be noted that the fluctuation is considerably smaller than that calculated for the Schott effect, which result was also found by Hafstad when testing the FP-54 tube designed especially for d.c. amplification.

PRACTICAL AMPLIFIER

In order to give an idea of the practical value of an amplifier constructed in the above manner the graphs of Fig. 4 are reproduced. These data were obtained by amplifying a photoelectric current of known value with the UX 222 operated at floating grid. Instead of reading directly the deflections of the galvanometer in the plate circuit, the current through this instrument was

[3] L. R. Hafstad, Phys. Rev. **44**, 201 (1933).

kept at a constant value by manipulation of the screen grid potential, the alteration in this potential being taken as a measure of the change of the control grid potential. When large deflections are to be encountered in the galvanometer some method such as this is desirable otherwise the range of the amplifier is limited by the range of the galvanometer. It would, of course, be better to keep a constant control grid potential, but in this circuit there is no method of readily determining this quantity. The graphs clearly show that this type of amplifier is capable of precise measurement for currents as low as 10^{-15} amp. Other data obtained for a single curve but not reproduced here show absolute linearity of amplification between 10^{-15} and 10^{-12} amp. Currents of greater magnitude than 10^{-12} amp. have not been examined. The constants of the above amplifier were:

Filament voltage	1.2,
Screen grid voltage	12.5,
Plate voltage	3.0,
Voltage sensitivity	10^{-5} volt/div.,
Galvanometer sensitivity	10^{-10} amp./mm,
Grid impedance	10^{11} ohms,
Current sensitivity	10^{-16} amp./mm,
Minimum detectable current	2×10^{-16} amp. (observed Johnson effect),
Drift	6 mm/min. at full sensitivity of 10^{-16} amp./mm.

It will be apparent that this is an amplifier capable of really precise work in spite of its simplicity. An ordinary dry cell was used for compensation on the plate circuit and a motor car storage battery supplied the remainder of the energy.

Balanced Circuit

The sensitivity of a twin tube balanced bridge circuit is just one-half that of the above type because of the bridge arrangement about the galvanometer. The voltage sensitivity of the above amplifier was however 10^{-5} volt/mm

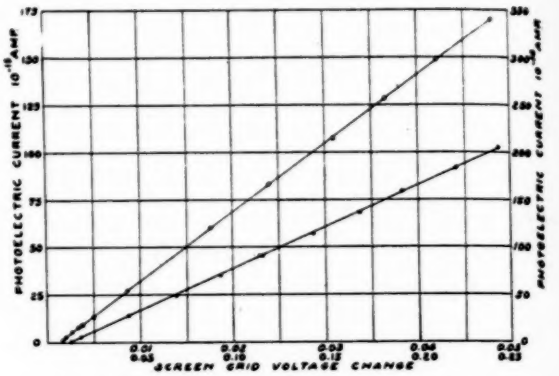

FIG. 4. These data show the value of a commercial screen grid tube employed as a direct-current amplifier at floating grid. In place of plotting the change in plate current resulting from the known photoelectric input current along the horizontal axis, the screen grid voltage change necessary to maintain a constant plate current is employed. It is not necessary to use this method of measurement as the plate current may be read directly if desired.

while the least detectable voltage with the grid floating is 2×10^{-5} volt, because of the irregular fluctuation, hence the use of a bridge circuit in this instance would not entail any loss in working sensitivity and would, of course, result in considerable increase in stability.

In considering the fluctuations introduced into such circuits by irregularities in supply batteries, it is a matter of interest to record that we were able to balance commercial radio tubes in the two-tube bridge circuit and obtain absolute freedom from irregular fluctuations at a sensitivity of 2×10^{-6} volt, provided no input resistor was employed. The plate potential in this case was 18 volts which precluded the use of such an amplifier for small current measurements, since such a high potential considerably reduces the input impedance. In these tests we found as before that on an average about three tubes out of twelve were stable.

This work has been carried out with the financial assistance of the International Cancer Research Foundation in the Radium Laboratory of the Manitoba Cancer Relief and Research Institute, established in the Department of Physics, University of Manitoba and the authors would like to express their thanks for the courtesies of these institutions.

Magnetic Hysteresis at Low Flux Densities

W. B. ELLWOOD, *Bell Telephone Laboratories*

(Received March 28, 1935)

The energy loss per cycle in a ferromagnetic material subjected to small alternating fields is sometimes separated into three parts; the first due to eddy current loss, the second to hysteresis presumed to follow Rayleigh's laws at these flux densities. The origin of the remainder is unknown and is the subject of much controversy; it has been variously termed "magnetic viscosity," "after effect" and "square law hysteresis." In studying energy loss in a ring of compressed iron dust, hysteresis loops have been measured ballistically by a new method with a relative error in B_m as low as 0.01 percent. The range in maximum flux density is from 2 to 100 gauss. The loops are lenticular and very slender, B_m being about 1500 times the remanence for the smallest loop. The smaller loops are at flux densities considerably below those investigated by Rayleigh. His findings as to variation of area, of remanence, and of permeability with loop amplitude are confirmed and extended through the new range of flux densities, though the shape of the loops is not as simple as that he proposed. The energy loss per cycle is proportional to B_m^3 while the remanence is proportional to B_m^2. The ballistic measurements have been compared with a.c. bridge measurements on the same specimen. The loss of unknown origin is not included in the hysteresis loss measured ballistically. Comparison is made between the third harmonic induced voltage computed by a Fourier series analysis of the ballistic loops and the harmonic actually generated by the specimen. Agreement is found between the measured and the computed values. Possible explanations of the discrepancy between the ballistic observed energy losses and a.c. findings are discussed.

INTRODUCTION

Historical background

Forty-seven years ago Lord Rayleigh[1] made his celebrated measurements on the properties of an iron wire at low fields with the aid of a magnetometer. He determined the shape of hysteresis loops for which the flux density at the tip B_m was as small as 30 gauss, and showed that within the limit of error the loop was described by a quadratic function of the field (see Appendix I). Since then Weiss[2] and more recently Wittke[3] have used ballistic methods, which have not greatly exceeded Rayleigh's measurements in sensitivity and accuracy.

Today the a.c. bridge employed in conjunction with high gain amplifiers allows one to investigate the energy losses when B_m is considerably less than that investigated by Rayleigh. Such measurements have been described in connection with papers by Speed and Elmen,[4] and Shackelton and Barber[5] on the properties of loading coil cores. Jordan[6] has shown that the energy losses per cycle measured in this way can be separated into three parts; one can be identified with eddy current loss; the second part, proportional to the cube of the maximum flux density [B_m^3 term], can be interpreted as hysteresis obeying Rayleigh's cube power law;[1] the remainder, proportional to the square of the flux density [B_m^2 term], has been the subject of much controversy as to its origin and even as to its existence. It has been called magnetic viscosity, after effect, initial or square-law hysteresis, or simply supposed to be due to the cumulative error in the bridge measurements. Jordan's opinion was that the additional loss was due to a time lag in magnetization other than that due to eddy-currents and analogous to viscosity.

Gans[7] has pointed out that the presence of the B_m^2 term in the a.c. data may mean that Rayleigh's law is modified at sufficiently low fields to include a B_m^2 term in addition to the B_m^3 term in hysteresis loss.

Peterson[8] has recently extended Rayleigh's expression to include terms of higher powers and has been able to evaluate the harmonics generated by the hysteresis loop, but his analysis includes no terms lower than the third power of H_m in the expression for the energy loss per cycle (Appendix I).

[1] Lord Rayleigh, Phil. Mag. [5] **23**, 225 (1887).
[2] P. Weiss, Éclairage Électrique **8**, 436 (1896).
[3] H. Wittke, Ann. d. Physik [5] **20**, 106 (1934).
[4] B. Speed and G. W. Elmen, Trans. A. I. E. E. **40**, 596 (1921) (B dust).
[5] W. J. Shackelton and I. G. Barber, Trans. A. I. E. E. **47**, 429 (1928).
[6] H. Jordan, Elek. Nach. Tech. **1**, 7 (1924).
[7] R. Gans, Ann. d. Physik [5] **20**, 701 (1933).
[8] E. Peterson, Bell Sys. Tech. J. **7**, 762 (1928).

Wittke[9] has recently made a loss separation of data obtained with the a.c. bridge at frequencies as low as 12.5 cycles per second, and has confirmed the existence of the square-law term at these low frequencies.

Purpose of the present work

Because magnetic properties at flux densities of 10 and less are of interest in their application to the design of magnetic apparatus, it was considered important to test these various hypotheses by extending ballistic or magnetometric (d.c.) measurements into the range of the a.c. bridge measurements for comparison with them. In this investigation the properties of a compressed iron dust ring at maximum flux densities ranging from 2 to 115 gauss have been studied and the d.c. loss measurements have been compared with the a.c. loss measurements. Further, the harmonics obtained by a Fourier series analysis of the d.c. loops have been compared with the harmonics generated by the same specimen which were measured by a.c. methods.

Obstacles to satisfactory d.c. investigation

As has been pointed out by Peterson,[8] the usual ballistic method has not hitherto been as accurate as the a.c. bridge method of measuring the properties of magnetic materials at these low flux densities because of the extreme lenticular thinness of the loops. To obtain a conception of the difficulties arising from this source, it is necessary to realize that on the seven loops measured in this study, with a sixty-fold range in B_m the area varies more than 100,000 times, while the width of the loop varies about 4000 times. Fig. 1 shows the largest hysteresis loop of the family of loops investigated. It is in that region of flux density studied by Rayleigh. The smaller loops of this family are at flux densities sufficiently low so that the B_m^2 part of the loss is about equal to the B_m^3 part as measured by a.c. methods. Although the sum of these two losses amounts to only a few microergs per cm^3 per cycle at the lowest flux densities, nevertheless under operating conditions this small energy loss may amount to about 30 percent of the magnetic loss in a loading coil and therefore cannot be ignored in practice, although it is difficult to measure.

[9] H. Wittke, Ann. d. Physik [5] **18**, 679 (1933).

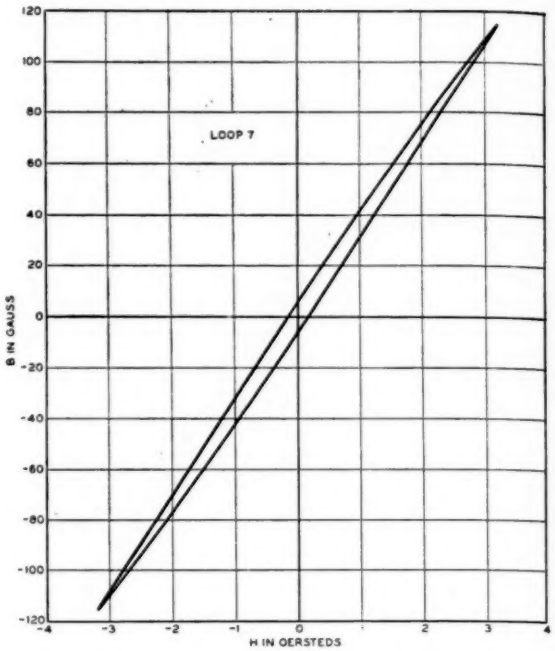

FIG. 1. The customary plot of the relation between B and H for the largest hysteresis loop investigated here. Compare with Fig. 2 and Fig. 4.

Rayleigh used a magnetometric method to obtain the shape of the hysteresis loops of his specimen. Foster[10] has pointed out that the demagnetizing factor is not only a function of the shape but also of the magnetization of the specimen, and this may introduce errors and certainly introduces difficulties into the interpretation of the results obtained by the magnetometric method. On this account it has not been employed in this investigation.

The ballistic method itself suffers from two grave difficulties. The first is the lack of sensitivity of ballistic galvanometers commercially available; the second is that ballistic galvanometers, in general, integrate correctly only under special conditions which have been discussed in a previous paper.[11] As we shall see, since the width of the loop is proportional to the square of the maximum field strength, the systematic errors inherent in the galvanometer, together with the errors of reading the galvanometer deflections, soon conceal the true shape of the hysteresis loop for low fields, particularly when the customary

[10] D. D. Foster, Phil. Mag. [7] **8**, 304 (1929).
[11] W. B. Ellwood, R. S. I. **5**, 301 (1934).

measuring circuit is employed. It is further to be pointed out that "least-squares smoothing" of the ballistic data does not eliminate systematic errors arising from these causes, but only accidental ones. In order to obtain the greatest precision it is necessary that the galvanometer be employed as a null or partial deflection instrument in a suitable circuit. Hitherto, because of the errors of integration in the galvanometer itself, such schemes have not generally worked satisfactorily although it has been used with success by Weiss.

In this research a special galvanometer[11] was employed which has a sensitivity about 150 times as great as previously available ballistic moving-coil galvanometers and which has the necessary accuracy of integration required to operate as a null instrument.

Method of Measurement

Increase in precision over the customary ballistic method is obtained by employing the galvanometer to measure the difference between two impulses which are almost simultaneously delivered to it. One impulse is delivered by the secondary circuit of an air core mutual-inductance when the primary current is changed suddenly. The other impulse is delivered by the secondary winding surrounding the specimen in which a change in flux occurs when the primary current is changed. The two secondary circuits are in series-opposition with each other and are in series with the galvanometer. The primary currents in the air core mutual inductance and the specimen are supplied by the same battery.

Comparison of an air core mutual inductance and specimen

With this arrangement, when the primary currents are simultaneously reversed the galvanometer measures the difference between the impulse due to reversing the flux in the air core mutual inductance and that due to changing the induction in the specimen from tip to tip of its loop. If this difference is made zero, and if the galvanometer integrates correctly, there will be no galvanometer deflection and the specimen and air core are said to be balanced. Then, if the currents in the primary windings of both the air core and the specimen are changed simultaneously and in the same ratio (to give any desired value of field intermediate between the tip values) the galvanometer will measure directly the difference in B, at the selected value of H, between the loop and the straight line drawn through its tips. This difference will hereafter be referred to as ΔB (see Fig. 2, curve a). For convenience in what follows, we shall plot ΔB against H directly as shown in Fig. 2, curve b. ΔB added to the corresponding heavily dotted ordinates will produce the loop plotted in the ordinary way. The dotted ordinates can be computed from the primary current in the mutual inductance.

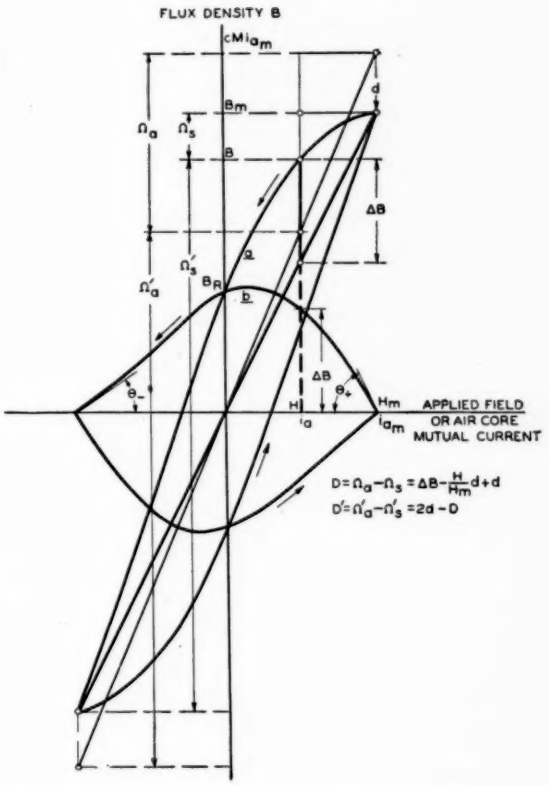

FIG. 2. The B–H plane showing the impulses delivered to the galvanometer, the primary field currents and the flux density together with the relationship between the new ΔB *vs.* H curve and the customary B *vs.* H curve.

In order to facilitate the description of the method and its application, all galvanometer impulses and their corresponding deflections will be considered hereafter as reduced to their

equivalent displacements in the $B-H$ plane as shown in Fig. 2; that is, the galvanometer deflection which would correspond to the change in flux of the specimen $B_m-B=\Omega_s$ will be considered as reduced to Ω_s units, where Ω_s is proportioned to the impulse delivered to the galvanometer by the change in flux in the specimen. Likewise the air core mutual inter-linkages will be considered equivalent to a flux density in the specimen equal to $cMi_{a(m)}$ where M is the mutual inductance of the air core, $i_{a(m)}$ its maximum primary current, and c is a constant so chosen that when the air core and specimen are balanced $cMi_{a(m)}=B_m$. If unbalanced, we have instead the relation $cMi_{a(m)}=B_m+d$, where d is the amount of the unbalance as shown in Fig. 2. A change in current $i_{a(m)}-i_a=\Delta i_a$ in the mutual primary is equivalent to a change in flux $cM\Delta i_a=\Omega_a$ in the specimen, and the difference between the specimen and the mutual at any other point than B_m is given by $D=\Omega_a-\Omega_s$.

The relation between D and ΔB is easily derivable from Fig. 2, and is shown there.

Principle of the method of single impulses

We have shown how the galvanometer is employed to measure the difference between a mutual inductance and a specimen. This difference is measured in terms of the net impulse proportional to it which causes the galvanometer to deflect. If the sensitivity of the galvanometer is such as to give a satisfactory deflection upon the application of the single differential impulse, it is possible to use the method outlined above without further refinement. The galvanometer is brought to rest after each deflection. The amount of unbalance (d in Fig. 2) between the mutual and the specimen at the tips of the loop is determined by reversing simultaneously the current in the primary of the mutual and in the specimen. The difference D between the mutual and the specimen at any value of field strength H may be obtained by changing simultaneously and in the same ratio the currents in the two primary windings so as to change H_m in the specimen to H. From these two galvanometer deflections and currents in the primaries of both air core and specimen the ΔB corresponding to that value of H may be readily computed.

Method of repeated impulses

In most of the loops studied in this analysis, the single deflection sensitivity of the galvanometer was not great enough. It was necessary to resort to the method of repeated impulses previously described[11] in order to obtain a suitable increase in sensitivity. By this means it is possible to determine the amount of unbalance (d, Fig. 2) between the air core and the specimen very accurately; when they are exactly balanced the galvanometer will not be set swinging even by repeated impulses in tune with its period.

To obtain points on the loop by the method of repeated impulses, it is necessary to modify Maxwell's method. Consider curve a of Fig. 2. Let us suppose that the balance between the mutual and the specimen is perfect at the tips of the loop, and the galvanometer is initially at its zero position. If, starting with an applied field H_m, we suddenly proceed as before to any desired field H less than H_m, the galvanometer will receive an impulse proportional to ΔB, as defined above, and will give a deflection. If, when the galvanometer passes through zero on its return the primary currents are again changed simultaneously and in the same ratio so that H becomes $-H_m$, the galvanometer will receive an impulse identical in magnitude with the first but opposite in sign; and since the damping of the galvanometer is purposely very small, the second deflection will be larger than the first and in the opposite direction. If at the third swing of the galvanometer, we proceeded from $-H_m$ to $-H$, the impulse would oppose the motion of the galvanometer, therefore it is necessary to wait at the tip of the loop until swing No. 4, when we proceed from $-H_m$ to $-H$; at swing No. 5, we go from $-H$ to $+H_m$ and again wait at the tip of the loop during swing No. 6. At swing No. 7 of the galvanometer the cycle is started anew. Repetition of this process a sufficient number of times will cause the galvanometer to build up to an ultimate deflection $D'_{2/3}$ which is proportional to ΔB. This complicated cycle of impulses applied to the galvanometer four swings out of six will be called hereafter 2/3 timing to distinguish it from Maxwell's method of repeated impulses, here called 3/3 timing, in which the

impulses are applied with each swing of the galvanometer.

It is evident that 3/3 timing may be employed if desired by switching from $+H$ to $-H_m$ to $-H$ every other swing of the galvanometer and from $-H$ to $+H_m$ to $+H$ for the alternate swing. The complicated switching involved and the short time available to perform the switching are regarded as sufficient objections to the complete 3/3 method.

If the balance is not perfect ($d \neq 0$ in Fig. 2) then the impulses D and D' are not equal and a correction must be applied for the unbalance.

It is necessary to multiply $D'_{2/3}$ as obtained by 2/3 timing by the factor 3/2 in order to express it in the same units as d which was obtained by 3/3 timing. This factor 3/2 may be derived from energy considerations and it has also been experimentally verified. The relationship between ΔB, D, D' and $D'_{2/3}$ and d may then be derived from Fig. 2.

Circuit and Manipulation Technique

Circuit

The circuit employed in these measurements is given in Fig. 3. It is a Maxwell mutual inductance bridge in which the positions of the galvanometer and the battery have been transposed. A switch S is used to reverse suddenly the current through the bridge; another switch S_1 shunted across a variable resistance R, allows the current to be reduced in both the air-core and the specimen primary windings simultaneously and in the same ratio. The resistances R_a, R_s and R_{a+s} are used to adjust the currents in the primary windings of both air core and specimen, so that the specimen primary current, i_s, may be held constant while the air core primary current, i_a, may be adjusted independently. Then upon reversal of both primary currents the flux interlinkages with the secondary windings s_a and s_s undergo changes nearly equal in magnitude but opposite in sign. The variable inductance L is inserted in series with the proper primary winding and is adjusted to make the time constants of both primary circuits the same, as nearly as possible. This is necessary if the peak current through the galvanometer, which flows when the primary currents are reversed, is to be kept small, this being one of the conditions for accurate integration.

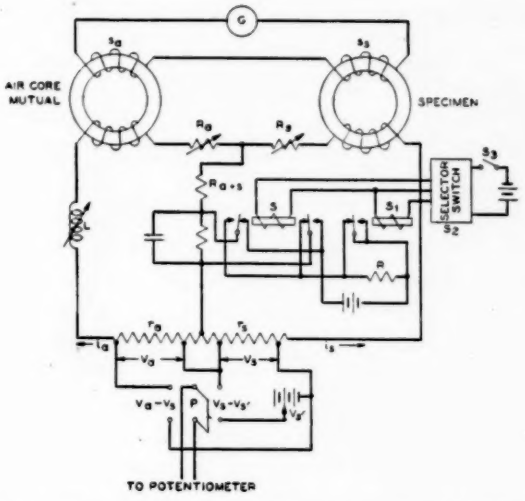

FIG. 3. The measuring circuit and associated switches.

Prevention of oscillations

The switch S is shunted by a resistance approximately equal to the resistance of the bridge circuit in parallel with a condenser of about 1/2 microfarad. The purpose of this shunt resistance and condenser is to eliminate sparking at the switch contacts and to keep the time constants of the primaries of the specimen and mutual inductance from being changed too greatly by operation of switch S_1. Thus employed it prevents high frequency oscillations, which have a demagnetizing effect, from being generated in the primary circuit.

Measurement of primary currents

The primary currents i_s and i_a are measured in terms of the voltage drops v_s and v_a across the resistances r_s and r_a, respectively. Because one scale division of the galvanometer corresponds to about 1 part in 100,000 of ΔB at $\Delta B = 10$, and since the potentiometer which was available to measure v_a and v_s was only accurate to 1 part in 10,000, it was necessary to provide switches s and p to allow the potentiometer to measure $v_s - v_a$. The value of v_s (and hence i_s) was held constant by holding $v_s - v_s'$ constant, where v_s' is the e.m.f. of a battery of standard cells.

Switching procedure and manipulation

In order to get from H_m to any desired H, it is only necessary to operate switches S and S_1 in the proper order. For the upper branch of the hysteresis loop, values of H between $H=0$ and $H=H_m$ are obtained by opening switch S_1, after having previously adjusted R to give the right current. Values of H between $H=0$ and $H=-H_m$ are obtained by operating switch S_1 to give $+H$ followed immediately by a reversal of switch S. An analogous procedure is used to obtain points on the lower branch of the hysteresis loop. The order in which switches S and S_1 are operated is automatically determined by a selector switch[12] S_2, which is put in charge by first closing and then opening a switch S_3. The selector switch then operates S and S_1 in the right order to produce the desired change in the field current necessary to obtain ΔB.

There are two additional adjustments: (1) The current i_s is held constant and i_a is adjusted so that upon reversal the galvanometer gives only a very small deflection; (2) the time constants of the primary circuits are then adjusted to be very nearly equal by substitution of a telephone receiver for the galvanometer and adjustment of the value of L to produce a minimum of sound upon reversal of the primary currents.

By repetition of adjustments (1) and (2) a few times, a satisfactory approximation to a perfect balance can be obtained and the current through the galvanometer will at all times be small.

The value of d is determined by starting with the maximum positive primary current and reversing to the maximum negative current. The deflection of the galvanometer due to this operation is proportional to $2d$ (see Fig. 2). Other points on the loop are obtained by starting again with H_m and dropping suddenly to any desired H by proper manipulation of switches S and S_1. The galvanometer will give a deflection proportional to D (Fig. 2) and from these deflections and the primary currents the values of ΔB, B and H may be computed.

If the single deflection sensitivity of the galvanometer is insufficient to measure ΔB conveniently, the method of repeated impulses must be employed. Because the increase in sensitivity due to this method is about 30 times the sensitivity obtained with the single deflection method, corresponding refinements are necessary. The value of d is obtained as before except that now we employ 3/3 timing to obtain a larger deflection for d, and $D'_{2/3}$ is obtained by 2/3 timing.

The values of H and $H_{\max}$ are determined by computation from the readings of the potentiometer and the e.m.f. (v_s') of the standard cells. The value of current i_s corresponding to H (and measured as v_s-v_s') is adjusted to a constant value during the time that the specimen remains at the tips of the loops. Other values of H are measured by reading the currents corresponding to them immediately after they have been established.

It is essential to the method of repeated impulses that the impulse be given to the galvanometer when it is passing through its zero position. It is possible to operate switch S_3 by hand so as to insure this being done. However, it is more convenient to employ light reflected from the galvanometer mirror itself to actuate a photo-cell and amplifier. The amplifier then operates the relay switch S_3 automatically as described before,[11] and the operator is relieved of the strain of closely watching the galvanometer for long periods of time. For each observation the galvanometer is read after 50 periods.

In actual practice it was found that the value of d fluctuated somewhat, probably because of changes in room temperature. Therefore, it was necessary to measure it before and after each determination of D or $D'_{2/3}$ and to use the average value of these two readings.

With the above scheme it is necessary that the switches S and S_1 be free from chatter. To this end the switches were specially constructed with contacts consisting of a fine copper wire and a pool of mercury in a glass tube. The copper wire was moved rapidly and over a considerable distance normal to the mercury surface to make or break contact.

The Specimen and Mutual Inductance

The specimen studied in this investigation was a toroidal core made of rings of compressed iron dust,[4] having an inside diameter of 7.86 cm, a

[12] W. Fondiller, Bell Sys. Tech. J. **9**, 237 (1930).

radial thickness of 2.71 cm and an axial height of 4.59 cm. Two windings, one of 120 turns and one of 1800 turns, carefully insulated from each other and from the core, were uniformly distributed around the circumference of the ring. The whole was enclosed, with a clearance of about one inch, in a permalloy box of $\frac{1}{4}$-inch wall thickness, to shield out stray magnetic fields.

Either winding of the specimen could be used as secondary. This allowed the large range of ΔB to be covered without the use of shunts in the galvanometer circuit.

The mutual inductance of 19 millihenries was wound on a wooden torus and consisted of two windings evenly distributed and insulated from each other. While it is not necessary that the mutual inductances of the specimen windings and of the air core windings be equal it is best that their ratio should not be greater than 3 : 1, because of the different amount of heating produced by the primary currents. This ratio was not exceeded in the windings here used.

Both specimen and mutual inductance are kept in a single copper shield which is grounded to protect them from vagabond currents.

Results

Fig. 1 shows the largest loop studied in this investigation, plotted in the customary manner. In Figs. 4 to 6, the values of ΔB instead of B are plotted against H for all of the loops measured. Accompanying each curve is the corresponding value of B_m determined from the current in the mutual inductance and the unbalance d. Since the height at the middle, $\Delta B_R (= B_R)$ and the extreme abscissas $\pm H_m$ are the same whether the loops be plotted this way or in the customary manner, no change in area occurs and this new method of plotting allows one to measure the area accurately with a planimeter. Then the energy loss is computed by the classical formula.

$$W = (1/4\pi) \oint H dB.$$

Some conception of the magnitudes involved may be gained by imagined plotting of the smallest loop No. 1 and the largest loop No. 7 on the same scale as the actual galvanometer deflections corresponding to the ΔB's measured in the smallest loop. If the scale were chosen so that the remanence of loop No. 1 were 13 milli-

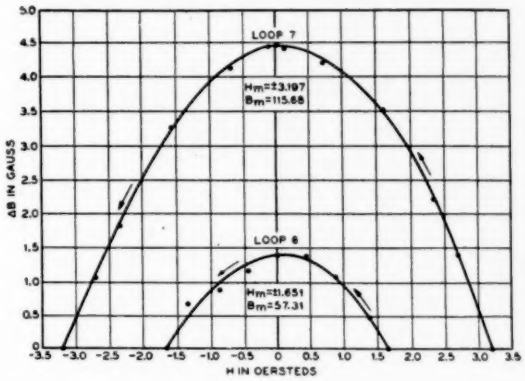

FIG. 4. The relation between ΔB and H for loops 7 and 6. Only half the loop is given, the other half is assumed symmetrical, see Fig. 2.

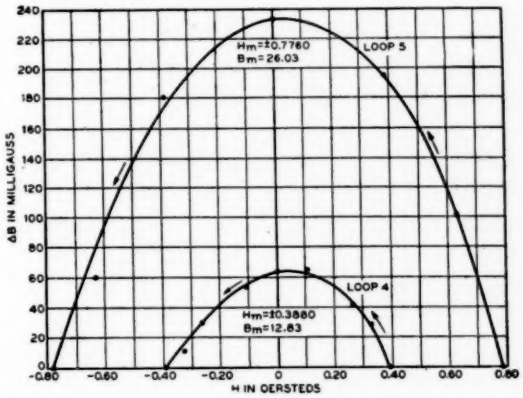

FIG. 5. The relation between ΔB and H for loops 5 and 4. Note change in scale from Fig. 4.

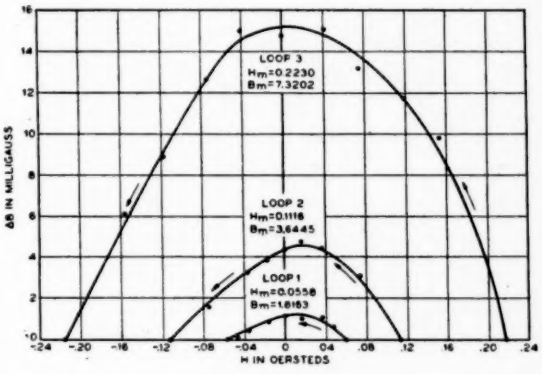

FIG. 6. The relation between ΔB and H for loops 3, 2 and 1. Note change in scale from preceding figure.

meters (the equivalent galvanometer deflection), the tip or B_m of the smallest loop would be about 22 meters above the H axis while the largest loop would cross the B axis 55 meters above the origin

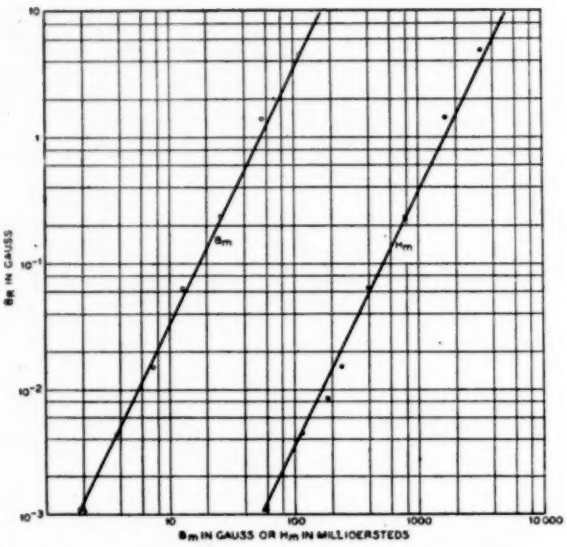

FIG. 7. The remanence B_R as a function of H_m and B_m. The straight lines represent simple quadratic functions.

and the tip of the loop would be at an altitude of nearly 1500 meters. For this reason no attempt has been made to plot B against H directly.

The results show that ΔB for any positive H is slightly greater than the ΔB for the negative value of H as plotted. This difference was not detected by Rayleigh; and Gans[7] and Wittke[3] assume it to be zero in their recent papers. This asymmetry, however, is believed genuine because there is nothing asymmetrical in the process of taking the points on the loop and all loops show the same asymmetry whether taken by the single or repeated impulse methods.

This series of loops is distinguished by the rapidity with which the remanence decreases as H_m decreases. It will be seen from Fig. 7, that the remanence plotted against H_m and also against B_m decreases as the square of either H_m or B_m in accordance with Rayleigh's findings. Attention is called to the logarithmic scale of the plot and the great range of remanence values which is approximately 4000 : 1. The fact that these results may be plotted equally well against either B_m or H_m is due to the fact that the slope of the $\mu-H$ curve is very small. The straight line is drawn to have the right slope for a simple quadratic relation and the closeness with which the points fall on the line attests the accuracy with which the remanence is proportional to the square of B_m or H_m. Attention is also called to

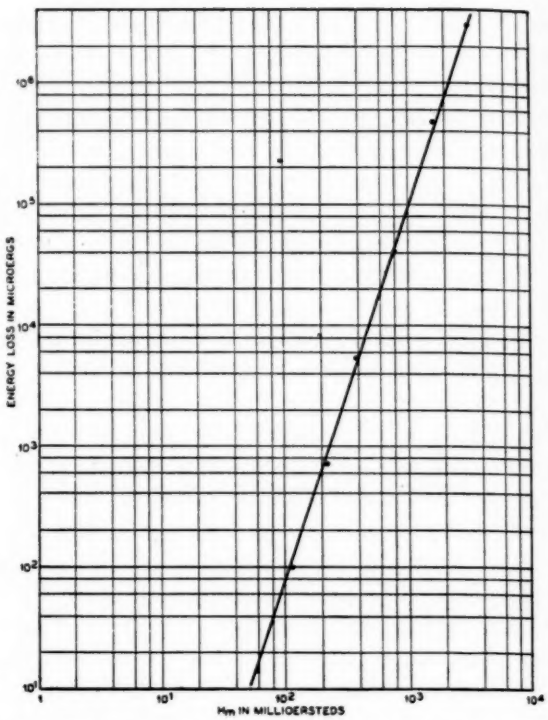

FIG. 8. The energy loss is proportional to the cube of the applied field.

the fact that no linear term is apparent in any systematic divergence from the straight line.

The energy losses obtained by measuring loop areas have been plotted as circles on a logarithmic scale in Fig. 8. The solid line is drawn to fit a cubic relation.

For comparison purposes, *alternating-current measurements* have been made on the same specimen by L. R. Wrathal and R. F. Squires of these Laboratories. Each has made his measurements on a different a.c. bridge using a different one of the windings described above. From their data separations of core losses have been made based upon the Eq. (1).

$$\Delta R/\mu Lf = 8\pi W/B_m^2 + 8\pi\gamma f, \qquad (1)$$

wherein ΔR is the a.c. resistance (R_f) minus the d.c. resistance of the coil surrounding the specimen, in ohms; L is the inductance of the coil in henries; μ the permeability of core material; γ the eddy current coefficient; f the frequency of magnetizing current, in cycles/sec.; B_m the maximum flux density in gauss at which the coil is operating; and W the magnetic core loss other than eddy currents, in ergs per cc per cycle.

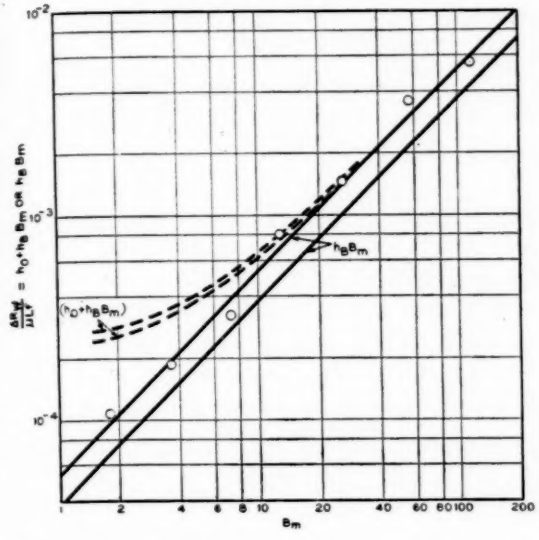

FIG. 9. The equivalent a.c. resistance ΔR_W computed from the ballistic data, plotted as circles, compared with the measured a.c. data obtained with different bridges and windings. The values of the a.c. B^3 term fall between the solid lines while the sum of the B^2 plus the B^3 term falls between the broken lines.

Experimentally from the bridge measurements

$$\Delta R_W/\mu Lf = 8\pi W/B_m^2 = h_0 + h_B B_m, \qquad (2)$$

where ΔR_W is the part of the effective resistance not due to eddy currents.

The values of $\Delta R_W/\mu Lf$ from Eq. (2) using Squires' and Wrathal's data have been plotted on a logarithmic scale against B_m and are included within the broken lines shown in Fig. 9. The portion $h_B B_m$ as determined by each observer is included between the solid lines. The circles give the ballistically measured hysteresis loss converted into $\Delta R_W/\mu Lf$ by the preceding formula, plotted against the corresponding values of B_m. The points plotted from the ballistic data fall approximately within the region bounded by the solid lines and hence it is to be concluded that only the term $h_B B_m$ is accounted for by the area of the ballistic loop; in other words, no B_m^2 term exists in the law relating W to B_m, if W is the hysteresis loss determined by the ballistic measurements above. Thus, the portion of $\Delta R_W/\mu Lf$ which is due to hysteresis as measured by the ballistic loop, approaches zero as B_m approaches zero, as indicated by the trend of the points plotted from the ballistic data. The intercept h_0, from which Gans infers the presence

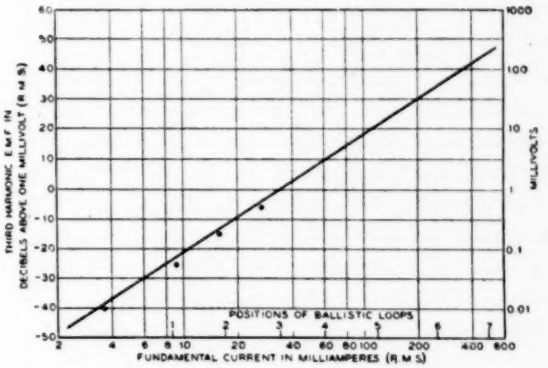
THIRD HARMONIC E.M.F. IN DECIBELS ABOVE ONE MILLIVOLT (R.M.S.)
MILLIVOLTS
POSITIONS OF BALLISTIC LOOPS
FUNDAMENTAL CURRENT IN MILLIAMPERES (R.M.S.)

FIG. 10. The third harmonic e.m.f. generated by the specimen as a function of the fundamental current, plotted as circles. The solid line represents the values computed from the ballistic data.

of a B_m^2 term in the hysteresis loss, is not accounted for by the ballistic data, and unless the dynamical hysteresis loop differs from the static loop the inference must be drawn that h_0 is due to some other mechanism than hysteresis.

R. M. Kalb and M. E. Campbell of the Laboratories have made measurements on the harmonics generated by this specimen throughout the range of flux densities studied. They have also computed the harmonics by a Fourier series analysis of this family of loops which I have measured ballistically. They find experimentally that the third harmonic voltages are proportional to the square of the fundamental current and that they agree in magnitude with the values calculated from the Fourier series analysis of the family of ballistic loops. Fig. 10 shows both the measured and the calculated values of third harmonic e.m.f. plotted on a logarithmic scale, for the 120-turn winding described above. The circles are the observed values while the straight line (which has a slope of 2) gives the values computed from the ballistic loops. The significance of the qualitative agreement between the observed and calculated results will be discussed later.

The value of α calculated for the seven ballistic loops by means of Eq. (6) in Appendix I, is 0.81 ± 0.05 and exhibits no systematic variations with B_m. The value computed from Eq. (3) varies between 1.7 and 1.1 for the seven loops which were measured over a period of several months with varying room temperatures. When data were taken in one day under reasonably

constant conditions Eq. (1) gave $\alpha=0.97\pm0.11$ for the lower fields. The values of α computed from the change of inductance with current are 1.03 and 0.94 for the two sets of a.c. data. The value of μ_0 for data taken in one day is 32.3. After due consideration of the fact that room temperature was not controlled it is concluded that α is the same and is constant for both the a.c. and d.c. measurements within experimental error.

Discussion

Comparison of d.c. results with Rayleigh's laws

The four relations, Eqs. (3) to (6) given in Appendix I, are commonly considered to hold in the region of flux densities under consideration. They are referred to as Rayleigh's laws and although Eq. (6) (called Rayleigh's cube power law) follows from the integration of Eq. (4) around a cycle, it was never expressly stated by him.

The results we have obtained at these low flux densities are in agreement with the laws determined by Rayleigh from observations made by him at higher flux densities, except for the slight asymmetry of the loops. This does not affect the validity of Rayleigh's relations given in Eqs. (3), (5) and (6).

The ballistic loops determined here depart slightly from the symmetry called for by Eq. (4) although the energy loss per cycle is still proportional to H_m^3. The value of the constant coefficient α is given within experimental error by any of Rayleigh's relations subject to the restriction that in the case of Eq. (3) α is obtained from the values of B_m and H_m observed in a single day. (See data.)

The tangent to the ΔB *vs.* H curve at $\pm H_m$ makes an angle θ (see Fig. 2) with the H axis. For a Rayleigh loop $\theta_+=\theta_-$ and is given by Eq. (7). It is found in these loops that θ_+ is given by Eq. (7) while θ_- is less than that.

The remanence ΔB_R is proportional to H_m^2 in accordance with Eq. (5). In order to account for the B_m^2 term added to the Rayleigh loop by Gans, the remanence ΔB_R for loop No. I would have to be three times as large as it is observed ballistically to be. Such a discrepancy cannot be accounted for by any known systematic or accidental errors in these ballistic measurements.

Comparison of a.c. and d.c. data

Before accurate ballistic measurements were made in this region, the a.c. data might have been explained in several ways some of which will be discussed here.

First. As Gans has assumed, Rayleigh's cube power law for hysteresis may be modified by adding to the Rayleigh parabolic loop a second parabolic loop of the proper size to account for the B_m^2 term of the a.c. data. See Appendix II. The coefficient of the B_m^3 term in the Gans law is not related to the coefficient of the B_m^2 term nor to the slope of the permeability curve. The assumption of a parabolic addition to Rayleigh's loop is not the only possible one. The addition of other forms such as an ellipse or a triangle may quite possibly account for the B_m^2 term. The additional loop in any case has the property of retaining its shape; that is, $B_R/B_m=$a constant as B_m is varied, whereas in the Rayleigh loop B_R/B_m approaches zero as B_m approaches zero.

The ballistic data presented here definitely show that this supposition is untenable. There is no modification of the ballistic or quasi-static hysteresis loop sufficient to account for the B_m^2 term required by the a.c. data.

Second. As Jordan has supposed, the B_m^2 term may be due to lag not due to eddy currents but analogous to viscosity which causes the dynamic loop to differ from the quasi-static or ballistic loop which follows Rayleigh's law. The chief objection to this viscosity analogy is that viscous forces usually produce dynamical loops which change their area with frequency while B_m is held constant. By the separation of losses, the dynamical loop as inferred from the a.c. bridge measurements for any given B_m does not change its area appreciably with frequency over an extraordinarily large range. In order to have this property the coefficient of viscosity would have to vary inversely with frequency which arbitrary assumption has no plausible explanation at present. The existence of a time lag other than eddy currents is still a matter of controversy,[13, 14] but even if the fact is established beyond doubt it is difficult to see how this lag

[13] R. M. Bozorth, Phys. Rev. **32**, 124 (1928).
[14] A. Mitkevitch, Comptes rendus de l'Acad. U. S. S. R. **1** (9), 534 (1934).

would produce a loop with nearly constant area over such a large range in frequency (12 to 4000 cycles per sec.).

Third. The B_m^2 term may originate in some process, neither magnetic hysteresis nor viscosity, which causes the dynamic loop to differ from the static one by the required term. Some possible processes will be discussed later.

The last two suppositions are not distinguishable from each other by any quantitative test yet available. The agreement of the observed third harmonic e.m.f. plotted against the fundamental current with the values computed from the ballistic loops is of significance only insofar as it shows that whatever causes the B_m^2 term in the a.c. loss data does not appreciably change the third harmonic of the dynamic loop from that predictable from the static loop. E. A. Neumann[15] has discussed the harmonics of a loop of the Gans type and concluded that the third harmonic e.m.f. of such a loop would not be simply proportional to the square of the fundamental current (as in a Rayleigh loop and as observed here) but would contain a linear term which would become more important as the current decreased.

In other words the third harmonic of a Gans loop plotted on a logarithmic scale against i_s would have a slope of 2 for high values of i_s and a slope of 1 for low enough values. Neither the observed nor the computed values of third harmonic e.m.f. generated by this specimen when plotted logarithmically show any trend away from the straight line of slope 2. It may therefore be inferred that the dynamic loop, if it differs from the static loop, does so by additions which only slightly affect the lower harmonics. The ellipse is a plausible addition of this sort since it would add nothing to the harmonic e.m.f.'s although it would account for the difference in area between the dynamic and static loops.

To assume such an elliptical addition to the static loop does not explain it. A suitable and probable mechanism must be invented and, if possible, the existence of the ellipse should be verified by a comparison of the dynamic and static loops. Jordan has given one possible explanation; others are also possible, though all are difficult to verify experimentally.

[15] E. Neumann, Zeits. f. Physik **89**, 308 (1934).

Possible explanations for the B_m^2 term (not quantitatively tested)

In seeking explanations for the B_m^2 term of the a.c. data one must keep in mind the nature of the loss to be explained. The observed loss (ergs/cm^3/cycle) is like eddy current loss and viscosity in that it is proportional to B_m^2 and is unlike them if it is, as generally believed, independent of frequency over a large range. Furthermore the B_m^2 term does not seem to contribute to the third harmonic e.m.f. generated by the specimen nor to the area of the ballistic loop.

Among other explanations, the B_m^2 loss may be conceived of as elastic hysteresis obeying Kimball's law,[16] with magnetostriction providing the necessary coupling between the elastic and magnetic variables. R. L. Wegel by mechanical vibration methods[17] has found the elastic hysteresis constant of this material to be very large (about that of lead) agreeing with the presence of a nonmetallic insulating cement between the particles of iron dust. From this constant (2×10^{10}ergs/cm^2/cm^3/cycle) it appears that a strain of the order of 10^{-8} at a B_m of 2 would account for the B_m^2 term of the a.c. data yet it is highly improbable that it would modify the ballistic loop. In the absence of a knowledge of the magnetostriction curve at these low fluxes it seems impossible to discuss this any further than to say that it is a possible explanation.

E. P. T. Tyndall[18] has commented on the necessity of taking account of the energy dissipated by the eddy currents induced by the sudden changes in flux occurring with every sudden jump of the individual magnetic domains. This is to be distinguished from the eddy currents produced by the average continuous change in flux customarily assumed. On the assumptions that the average size of a domain varies as $B_m^{3/2}$, that its relaxation time is of the order of 10^{-4} seconds, that its volume at $B_m=2$ (assumed to be a cylinder with its length equal to its diameter) is about 10^{-18} cm^3, L. A. MacColl has made an approximate computation which indicates that the energy loss from this cause may account quantitatively for the B_m^2 term in the a.c. data.

[16] A. L. Kimball and D. E. Lovell, Phys. Rev. **30**, 954 (1927).
[17] R. L. Wegel and H. Walther, Physics **6**, 141 (1935).
[18] E. P. T. Tyndall, Phys. Rev. **24**, 439 (1924).

Such a loss would not contribute to the ballistic loop yet would give a loss per cycle of the dynamic loop which would be independent of the frequency provided the reciprocal of the relaxation time is small compared to the highest frequency employed. The assumptions made require experimental verification but in the absence of quantitative measurements are not too improbable.

Whereas it is difficult to justify an elastic hysteresis great enough to account for the B_m^2 term in the a.c. data (for 10^{-8} may be greater than the actual magnetostrictive strain were it possible to observe it), in the case of the Barkhausen eddy current loss the chief difficulty is to make the computed loss small enough (because both a larger particle or a shorter time would increase the energy loss). Both these phenomena are presented here merely as intriguing possibilities which have not yet been put to a more rigorous test because of the experimental difficulties involved.

Effect of harmonics on the energy loss as measured by the a.c. bridge

In the preceding discussion a fundamental question has been ignored. Does the energy loss involved in the harmonic currents (which ultimately must come from the fundamental frequency current and e.m.f.) constitute an appreciable fraction of the fundamental energy loss, enough to account for the B_m^2 term? The answer to this question depends upon the experimental fact that for sufficiently low flux densities the harmonic e.m.f.'s are experimentally proportional to the square of the fundamental current as seen in Fig. 10 and hence the harmonic energy losses (R_f and R_{harmonic} assumed approximately constant) are proportional to the fourth power of the fundamental current i_f. The ratio of the harmonic power loss, $(ci_f^2)^2/R_{\text{harmonic}}$, to the fundamental power loss, $i_f^2R_f$, for any given frequency becomes negligible as i_f approaches zero, hence the error involved in neglecting the harmonic power loss is negligible. Hence it is not possible to ascribe the B_m^2 term to energy diverted from the fundamental current into harmonic channels.

Mechanical hysteresis model

In seeking an explanation for Rayleigh's cube power law itself, a mechanical hysteresis model made by F. S. Goucher[19] presents some striking analogies to magnetic phenomena. For example, in the region of small displacements the energy loss per cycle as measured by the area of the force displacement diagram is proportional to the cube of the applied force, analogous to Rayleigh's law. From this model the inference may be drawn that Rayleigh's cube law is the result of either mechanical or magnetic propagative action; that is, one domain changes, then one of its neighbors, and so on. This mechanical model does not give an exact picture of the magnetic process yet it provides an interesting suggestion concerning the processes involved in the cube power law of magnetic hysteresis.

The progress of this investigation has depended upon the cooperation of so many individuals that it is impossible to make an acknowledgment of my indebtedness to each and every one. Nevertheless I wish especially to thank Dr. O. E. Buckley for his continued interest in this investigation, Dr. R. M. Bozorth for much helpful counsel and discussion and Professor L. W. McKeehan for valuable comment.

Appendix I

Rayleigh's laws

The permeability $\mu=\mu_0+\alpha H_m$ where $\pm H_m$ (3)

is the *maximum* field applied cyclically and μ_0 is the initial permeability. α is equal to $d\mu/dH_m$, a constant when αH_m is small.

The hysteresis loop $\Delta B=\frac{1}{2}\alpha(H_m^2-H^2)$ (4)

The remanence $B_R=\frac{1}{2}\alpha H_m^2$. (5)

The energy dissipated per cycle (ergs/cm^3)

$$W=(1/3\pi)\alpha H_m^3 \quad (6)$$

$$\tan\theta=\alpha H_m. \quad (7)$$

Appendix II

The Jordan-Gans law

$$W=(\lambda/2\pi)H_m^2+(2\nu/3\pi)H_m^3 \quad (8)$$

where 2ν is not necessarily equal to α, and λ is a constant.

$$B_R=(3\lambda/4)H_m+\nu H_m^2. \quad (9)$$

---

[19] F. S. Goucher, Phys. Rev. **45**, 743 (1934).

High Frequency Conductance of Pyrex Glass in the Presence of Vapors

W. M. ROBERDS,* *University of Kansas*

(Received October 22, 1934)

The electrical conductance of "Pyrex" brand glass 774 was measured at frequencies between 40 kc and 1000 kc in the presence of ethyl alcohol vapor and water vapor. Data were taken at 50°, 65°, 79° and 107°C. The relations between conductance, degree of saturation, and frequency were found to be of the same form at all temperatures. There is a distinct discontinuity in the curves of conductance *vs.* frequency at about 500 kc. Vapor pressures of alcohol up to 85 percent of saturation cause no change in the conductance of the test piece. However, above this degree of saturation the conductance increases rapidly with pressure, becoming very high if condensation occurs. Conductance decreased with increasing current unless the test element was aged in the vapor several hours. Surface conductivities for both alcohol and water vapor are computed. Those for water vapor agree, well within the limits of error, with the results found by Yager and Morgan. An unexplained resonance effect occurred when high currents were used to measure the conductance while the test element was in the presence of small amounts of either alcohol or water vapor. The effect shows the double resonance peak and many of the other characteristics of close coupling between oscillating circuits. However, the effect is in some way due to the energy absorbed in the test element in the presence of a minute amount of water or alcohol since either an increase or decrease of pressure will cause the disappearance of the phenomenon. It was impossible to produce the effect by the substitution of any combination of capacity and artificial leak.

INTRODUCTION

YAGER and Morgan[1] have investigated the surface conductance of Pyrex glass in the presence of water vapor at frequencies up to 100 kc. They found that both the volume conductance and the surface conductance increased rapidly with frequency. In the presence of water vapor at high humidities the surface conductance increased enormously.

Knowles[2] in work on the dielectric constant of ethyl alcohol vapor found deviations from the theory at high degrees of saturation which he showed were closely associated with leakage across the insulators of his test condenser. However, when he measured the d.c. resistance of his insulators, he found values of leakage which were far too small to explain the discrepancies.

Poulter and Wilson[3] have shown that at high pressures ethyl alcohol behaves much the same as water in its tendency to penetrate the surface layer of glass. Therefore, it seemed reasonable that the high frequency resistance of the Pyrex insulators in the presence of alcohol vapor might have been low enough to have caused Knowles' anomalous results. And since Knowles' work is only one of the many instances where Pyrex glass is being used as insulators in high frequency apparatus, it was deemed worthwhile to investigate the manner of variation of the conductance of the glass both dry and in the presence of alcohol and water vapors at frequencies up to 1000 kc. Also, such data would extend the work of Yager and Morgan and might shed more light on the process of adsorption. Since the possibility of covering a wide range of frequencies was more to be desired than very high accuracy a substitution method of resistance measurement, a modification of that described in the *Proceedings of A. S. T. M.*,[4] was used rather than a bridge method.

EXPERIMENTAL METHOD

The wiring diagram of the test circuit is shown in Fig. 1. The procedure consisted in tuning the circuit with the switch S closed and observing the current in G, then opening S, retuning, and bringing the current back to its previous value by increasing r_{1-2}. The leakage resistance across the test element was then equivalent to the change in series resistance r_{1-2}.

Letting z be the impedance of the circuit between points A and B, X the capacitative reactance, and R_l the leakage resistance between

*Now at the University of Arkansas.

[1] W. A. Yager and S. O. Morgan, J. Phys. Chem. **35**, 2026 (1931).

[2] H. L. Knowles, J. Phys. Chem. **36**, 2554 (1932).

[3] T. C. Poulter and R. O. Wilson, Phys. Rev. **40**, 877 (1932).

[4] Proc. A. S. T. M. **27**, 1003 (1927).

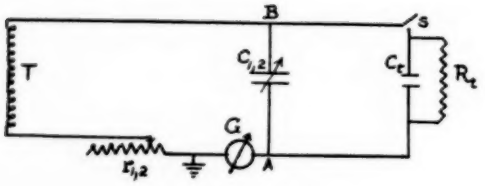

FIG. 1. The test circuit.

these two points we can write

$$Z=(R_tX^2-jR_t^2X)/(X^2-jR_t^2).$$

The real part of this expression is the equivalent resistance, while the complex part is the equivalent reactance.

If R_t is large as compared to X (which was the case in these investigations) the real part becomes X^2/R_t and the imaginary part merely X. If we let the change in the value of r_{1-2}, which is necessary to bring the current back to its first value, be designated as r then $r=X^2/R_t$ or $R_t=X^2/r$.

It is assumed here that the resistance between the leads and along the insulators in the tuning condenser are very large as compared to the capacitative reactance of the circuit. Calculations which are quite simple, even if tedious, show that although the neglected resistances are of the order of magnitude of R_t, still their effect is negligible so long as they are large compared to the capacitative reactance. For the resistances and reactances obtaining in this experiment the above relation is entirely valid.

It will be noted that the value of X is $1/(C_1+C_t+C_L)2\pi f$, where C_1 is the capacity of the tuning condenser when the circuit is tuned with S closed: C_t is the capacity of the test element, and C_L is the distributed capacity in the leads and coupling coils. Since eight different coils were used in order to cover the range of frequencies it was necessary to evaluate C_L for each of them. This was accomplished by plotting the capacities in $C_{1,2}$ against the corresponding values of $1/f^2$. The relation is a straight line whose negative intercept on the capacity axis is the distributed capacity in the circuit.

It will also be noted that, to a first approximation, $C_1+C_t=C_2$ where C_2 is the capacity of the tuning condenser which tunes the circuit with S open. The error incurred in the calculated value of R_t due to this approximation was never greater than 1 percent.

The total probable error was less than 5 percent for frequencies up to 500 kc and less than 10 percent at 1000 kc. This is, of course, less accurate than bridge measurements but the simplicity of this method along with the wide range of frequencies and resistances which may be covered compensate for loss of accuracy. And there is no reason why careful designing of the apparatus could not increase the accuracy of the method.

DESCRIPTION OF APPARATUS

The tuning condenser $C_{1,2}$ was a 1500$\mu\mu$f General Radio precision piece calibrated to 0.06$\mu\mu$f. The series resistance was a G.R. standard decade resistance box accurate to 1 percent up to 1000 kc. Several types of current measuring instruments were used for G. The most satisfactory instrument, for high currents, was a Weston Thermo-galvanometer with a range of 0–115 milliamperes. For low currents a Western Electric thermocouple type 20 AD was used in conjunction with a Weston microammeter, range 0–200 microamperes. With this latter combination currents of 6 milliamperes could be read accurately.

The coupling coils T were replaceable units of No. 20 copper wire wound on wood frames one foot square. The largest coil was wound with 75 turns while the smallest had only 5 turns, well spaced. The only solid insulators used outside the precision condenser were two hard rubber blocks used to mount the leads in a rigid position. The shortest leakage path over these blocks was about half an inch in length.

The test element is designated as C_t. A diagram of this piece is shown in Fig. 2. Several types of element and methods of construction were tried before this design was adopted. It was constructed in the following manner. A thick wall "Pyrex" glass tube $2\frac{1}{2}$ inches, outside diameter, and $5\frac{1}{2}$ inches long was grooved with 39 transverse grooves. These grooves were cut with a glass saw and were approximately 0.5 mm wide, 0.3 mm deep and were spaced 2 mm apart. In each groove was wrapped tightly one turn of No. 30 bare copper wire. These wires were connected into two groups so that alternate turns

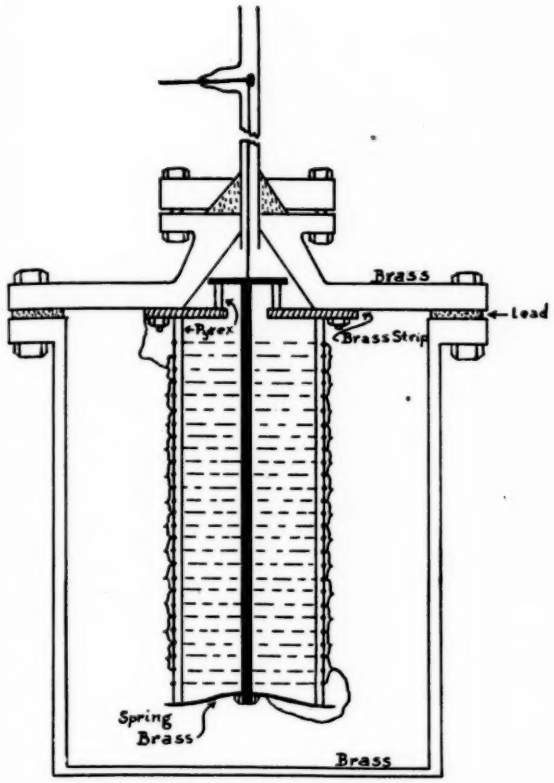

FIG. 2. Test chamber and element.

were in separate sets. Copper was then electroplated on the wires until the grooves were completely filled. The conductors were then approximately 1 mm in diameter. The element was mounted rigidly to the top of the vapor chamber as shown in Fig. 2.

The element was cleaned with chromic acid, washed thoroughly with a pure soap solution, then rinsed several times with distilled water and finally with alcohol.

The vapor system was similar to that used by Miles[5] and Knowles.[2] The vapor chamber could be evacuated to a high degree and then filled with pure alcohol vapor to any desired pressure up to 80 cm of Hg. The alcohol was dried by boiling with calcium oxide, distilled, boiled with metallic sodium and then refractionated. The chamber was immersed in an oil bath whose temperature could be controlled to 0.02 degree C.

In order to similate exactly the conditions obtaining in the experiments of Yager and Morgan one set of data on water was taken in the usual manner with only pure water vapor in the chamber. Then dry, clean air was admitted to bring the total pressure up to atmospheric and the same data repeated. The results in the two cases agreed, well within the experimental error. This would indicate that the pressure of air had no appreciable effect on the leakage.

The test circuit was calibrated like a wave meter for each of the coils used and the frequencies, at which the measurements were made, were determined from these calibration curves. Standard frequencies for the calibrations were obtained by beating the upper harmonics of the oscillator with the carrier frequencies of various broadcast stations.

EXPERIMENTAL TECHNIQUE

Considerable finesse had to be acquired in the experimental procedure before consistent results could be obtained. It was necessary to pump the chamber with a Hyvac pump for several hours before data were taken. The vapor was then admitted to the desired pressure and allowed to age 8 to 24 hours. With alcohol vapor in the chamber the conductance of the test piece varied with the current used. The data in Table I make this clear. Here i is the current through G in milliamperes and $1/R$ is the conductance in arbitrary units. The last reading shows that the high currents had a cumulative effect. About the same percentage of decrease is shown with high currents even after long aging. Due to the presence of this effect, the resistances were measured with currents less than 10 ma.

TABLE I. *Variation of conductance with current.*

FREQ. 485 kc SATURATION 97% (With no aging)		FREQ. 485 kc SATURATION 97% (After aging three hours)	
i	$1/R$	i	$1/R$
6.1	5.6	6.8	5.6
44.0	5.0	40.00	5.5
94.0	5.0	55.0	5.5
6.2	5.0	112.0	5.5

It was not necessary to pump out the chamber when the pressure was to be changed from a low to a higher value, but once a high pressure was used the chamber had to be pumped for several

[5] J. B. Miles, Phys. Rev. **34,** 964 (1929).

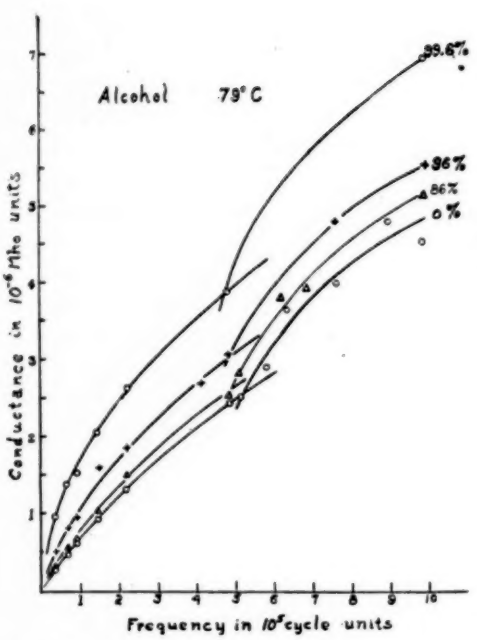

FIG. 3. Conductance of test element in alcohol vapor.

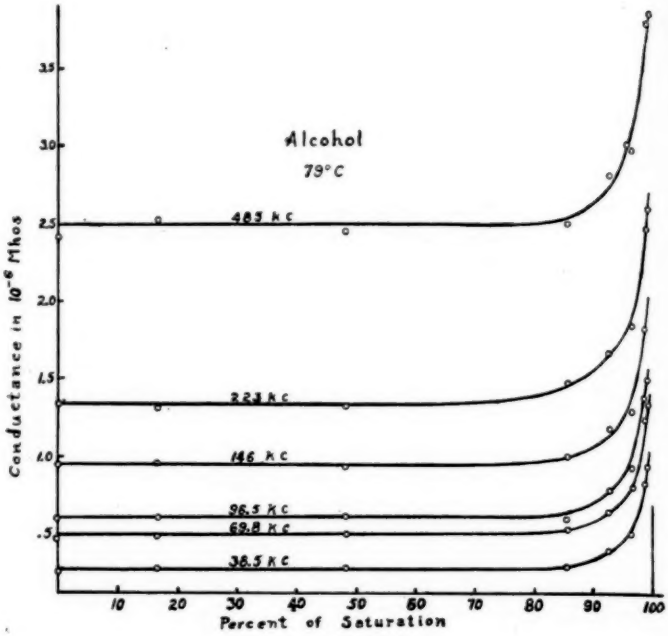

FIG. 4. Conductance *vs.* degree of saturation of alcohol vapor.

hours before measurements could be taken at a lower pressure.

When the vapor was admitted too rapidly, so that the saturation point was reached for even an instant, the conductance ran up enormously. Resistances of less than 10,000 ohms have been estimated under these conditions while the d.c. resistance of the element dry was of the order of 25 megohms. It is probably this too rapid influx of vapor and the consequent condensation which caused the anomalies in Knowles' results as Stranathan[6] has already reported.

Discussion of Results

The resistance of the test element was measured at seven different frequencies between 38 kc and 1000 kc, both dry and in the presence of ethyl alcohol vapor at degrees of saturation up to 99.8 percent. Similar data were taken at 51°C, 65°C, 79°C and some data were taken at 107°C. Some data were also taken on water vapor at 50°C. In the case of alcohol, the form of the curves of conductance *vs.* frequency and conductance *vs.* degree of saturation varied little, if any, with the temperature. Such curves taken at 79°C are shown in Figs. 3 and 4.

In the curves of conductance *vs.* frequency there is apparently a sharp break at about 500 kc. This is an effect in the dry glass and hence appears at the same point for all degrees of saturation of both alcohol and water. No explanation can be given, at this time, for such a discontinuity. Tests were made in an effort to find some characteristic of the apparatus which could cause it. However, measurements with different apparatus and at different frequencies than the seven commonly used, were consistent in showing the break. Careful inspection of the curves indicates that there may perhaps be another such discontinuity at about 100 kc; since this is questionable, smooth curves were drawn through this region.

The curves of conductance *vs.* degree of saturation show that alcohol vapor had to be more than 80 percent saturated before its pressure made any measurable difference in the conductance. On the other hand water vapor at 50 percent saturation causes an increase in conductance. Figs. 5 and 6.

[6] J. D. Stranathan, Washington Meeting of Am. Phys. Soc.; April, 1934; Phys. Rev. **45**, 741A (1935).

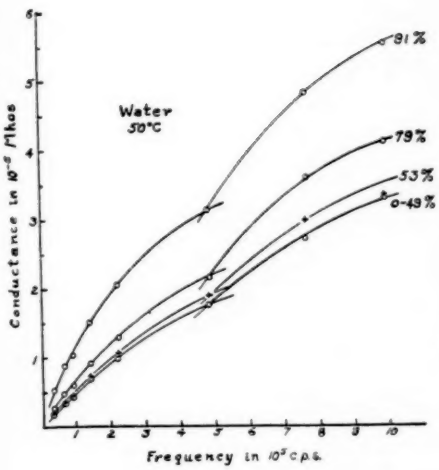

FIG. 5. Conductance of test element in water vapor.

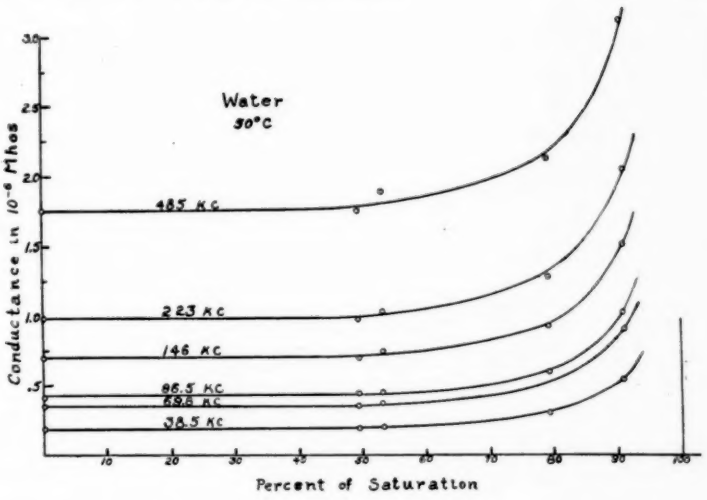

FIG. 6. Conductance *vs.* degree of saturation of water vapor.

CAPACITANCE OF SURFACE FILM

While the capacity of the test element increased with degree of saturation and decreased with increase in frequency these variations were so small that the probable error made further study of the variation unreliable.

VARIATION OF SURFACE LEAKAGE WITH FREQUENCY

The surface leakage is the difference between the total conductance in vapor and the conductance in vacuum. The curves in Fig. 7 show this difference plotted against frequency, for frequencies up to 500 kc. Above this frequency the experimental error made such differences meaningless.

VARIATION OF VOLUME CONDUCTANCE WITH TEMPERATURE

The volume conductance of the glass is the conductance in vacuum. In order to investigate the relation between volume conductance and temperature, additional data were taken at several temperatures other than those at which the vapor experiments were done. The results are shown in the curves of Fig. 8.

SURFACE CONDUCTIVITY

Surface conductivity is defined as the conductance of a square centimeter of surface when the electrodes are one centimeter apart. That is, $G=\gamma L/W$ where γ is the surface conductivity and G is the conductance of a strip L cm long and W cm wide, the electrodes being along the sides of the strip. In the test element used in the present experiments $L=537$ cm and $W=0.2$ cm. Therefore, $\gamma=3.73\times10^{-4}G$ mhos/cm square. From the curves of conductance *vs.* saturation (Fig. 4) G is obtained at any frequency and for any given saturation by subtracting the value of conductance on the horizontal part of the curve from the value on the curve at the desired degree of saturation. From the values of G thus obtained, the above relation between γ and G yields the surface conductivities given in Table II.

TABLE II. *Surface conductivities* (multiply each value by 10^{-12}).

	Alcohol (Temp. 79°C)			Water (Temp. 50°C)	
f	Sat. 90.0%	Sat. 94.2%	Sat. 98.7%	Sat. 90.0%	Sat. 90.3%
485 kc	52	149	429	168	477
223	49	145	377	131	373
146	45	90	295	97	280
96.5	37	86	242	71 (71.3)	213 (206)
69.8	34	75	224	63 (63.3)	190 (188)
38.5	26	56	187	52 (50.8)	134 (161)

The values in parentheses are from Yager's and Morgan's work. It is seen that in only one instance (the 38.5 kc frequency at 90 percent saturation) is there serious disagreement. This is

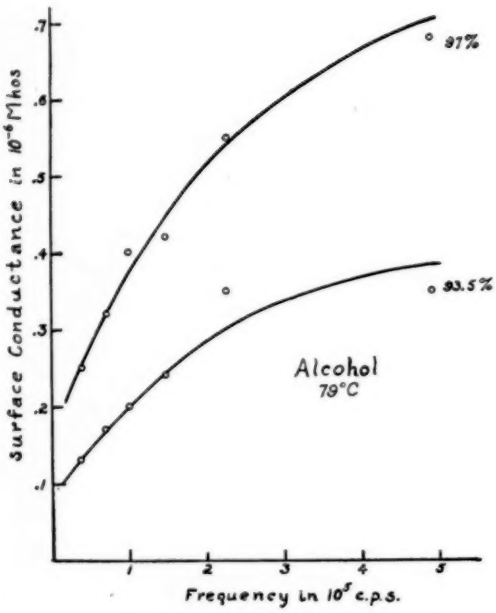

FIG. 7. Surface conductance in alcohol vapor.

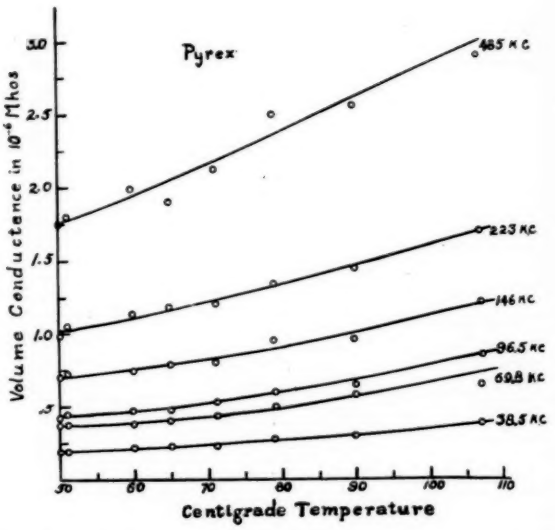

FIG. 8. Variation of volume conductance with temperature.

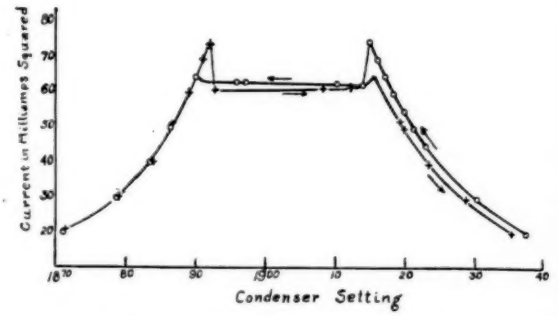

FIG. 9. Double resonance peaks in the presence of alcohol vapor.

obviously due to the error in the last point on the curve of conductance *vs.* pressure. The shape of 38.5 kc curve differs from the others due to the position of this one point. As was mentioned in the beginning, the data on water were taken principally to check with the work of other investigators and so only a few points were taken. However, in so doing, the work of these investigators is extended from 100 kc to 500 kc.

It might also be added that the agreement with the work of Yager and Morgan is, in general, better than the experimental error would warrant. The values of γ here listed for water are accurate to about 5 percent. The values for alcohol may be slightly better than that.

RESONANCE EFFECT WITH SURFACE FILMS

A peculiar phenomenon was observed when high currents were used in the test element in the presence of a slight amount of vapor. If currents of the order of 75 milliamperes flowed in the main circuit, i.e., through G while the vapor was being pumped out, at a certain low pressure (something less than one mm of Hg in the case of alcohol vapor) two distinct resonance peaks appeared as $C_{1,\,2}$ was tuned with S closed. A pair of such peaks is shown in Fig. 9. The arrow indicates the direction of the variation of the capacity. These peaks had all the characteristics of those observed when the coupling is too close between the oscillator and the test circuit. At first it was thought that close coupling must be the explanation. However, when the power in the oscillator was decreased without changing the coupling between the circuits the two peaks merged into the single peak normally present. Moreover, pumping the chamber for half an hour caused the doubling to disappear. The coupling could then be increased until the current reached the limit of safety for the galvanometer and the decade resistance box without causing the doubling to reappear.

Double peaks were never observed when S was open nor could they be produced in any other manner than that described above. When a good

vacuum had been attained in the test chamber an artificial leak of approximately the same value as that caused by the surface film was placed across the test element without producing the double peaks. Artificial leaks of greater and of less conductance were tried without success. Finally in place of the test chamber and element a condenser of the same capacity and leakage was substituted but still only one sharp resonance peak was observed.

Measurements of R_t with currents just below those required to produce the doubling were little if any different than the value of R_t in a vacuum.

The problem was then attacked from another standpoint. With the test element in the "double resonant" condition shunts of 2 to 10 megohms placed across it only lowered the current in G and did not otherwise modify the effect. When vapor was admitted to a pressure of about 2 cm of Hg the peaks merged into the single normal peak. The phenomenon appeared while the oscillator was radiating ten watts and the test circuit absorbing less than 0.25 watt.

The effect could be produced at almost any frequency although it appeared more readily at 70 and 100 kc. This was probably due to the fact that the coils used were of just the right inductance to produce the correct current distribution when $C_{1,2}$ was tuned. For example when the coupling coil No. 5 was in position and the circuit was tuned to 69.8 kc the double peak appeared as usual. However, when another coil having slightly less inductance than No. 5 was substituted for it and the circuit again tuned to the 69.8 kc frequency to the double peak could not be obtained. The oscillator and test circuit were then tuned to a slightly higher frequency and the double peak appeared under the usual circumstances.

A sensitive thermocouple along with a sensitive microammeter was placed in the circuit right beside the test element to measure the current in it while the total current was observed in G. The resistance of the thermocouple was 35 ohms so that its presence somewhat modified the circuit. However, the double peaks could be produced in the usual manner. The current built up simultaneously in both thermocouple and in G, as the condenser tuned the circuit, and as a peak was passed both currents "broke" together to some lower value. Such experiments indicate that the current in C_t was in phase with that in the main circuit.

The same doubling of the resonance peak appeared when water vapor was present. The peaks seemed a little more pronounced in the case of water and they appeared at a much higher pressure (around one cm of Hg). No satisfactory explanation for this phenomenon has been found. However, further work on it is contemplated.

The author wishes to express his thanks to Dr. J. D. Stranathan of this department who not only suggested the problem but outlined the method of attack and gave many suggestions as to the solving of difficulties. I am also indebted to Dr. F. E. Kester for reviewing of the work.

A Theory of Two-Dimensional Longitudinal and Flexural Vibrations in Rectangular Isotropic Plates

HAROLD OSTERBERG AND JOHN W. COOKSON, *Department of Physics, University of Wisconsin*

(Received September 11, 1934)

The differential equations of motion of a free, rectangular, isotropic plate are solved for the longitudinal and flexural cases upon the assumptions that the displacements are independent of one of the Cartesian coordinates and that the displacements parallel to this coordinate are negligible. The flexural and longitudinal cases are considered separately. The frequency expressions predict the effects due to mechanical coupling of two or more longitudinal modes or of two or more flexural modes. The effects of the lateral dimension of the plate upon the frequency of the longitudinal harmonics are also predicted. It is shown that in the longitudinal case only the odd harmonics of both of the modes in which the wave trains are propagated along X and Y, respectively, form a mechanically coupled system. Similarly, only the even harmonics of the flexural case form a mechanically coupled system. The law by which the displacements of two individual modes are combined to form two coupled modes is illustrated by means of photographs of interference patterns formed by a Y-cut plate of crystalline quartz which is vibrating flexurally. The mathematical methods which are developed in this paper can be employed in considering the coupling of the longitudinal modes with the flexural modes of vibration. The two-dimensional case here considered, i.e., that in which the displacements are limited to the XY plane, is of special importance since it can be shown that in quartz and tourmaline the differential equations of motion and the boundary conditions become identical in form to those of the rectangular isotropic plate when it is assumed that the displacements are restricted to the XY plane and are independent of z. The applications of this theory will be considered elsewhere.

INTRODUCTION

OUR present theories concerning longitudinal vibrations in an isotropic rectangular plate or bar do not properly take into account the components of displacement which are executed in the plane perpendicular to the direction of propagation. A correction for these lateral displacements, known as the Rayleigh correction, has been investigated by Giebe and Scheibe.[1] It was not found to account in a satisfactory manner for the anharmonic property of the overtones of an oscillating quartz plate. The observations of Giebe and Scheibe, who employ the glow method, and those made at this laboratory with the aid of several interference methods[2–5] point clearly to the conclusion that the lateral displacements are frequently associated with other modes of vibration. The manner in which this phenomenon of the mechanical coupling of two or more modes of vibration may be expected to affect the frequency of vibration has been described by Lack[6] and Hitchcock.[7] A satisfactory theory for longitudinal vibrations should predict the effects of mechanical coupling.

Theories of the flexural vibrations in rectangular isotropic plates have been advanced by Rayleigh,[8] Timoshenko,[9, 10] Madelung[11] and Goens.[12] The latter three theories can be shown to be nearly equivalent. They are more general than that described by Rayleigh in that they include the effects of shear.[9] These theories are essentially two-dimensional, i.e., it is assumed that the displacements are independent of one Cartesian coordinate and that the displacements along this coordinate are negligible. They do not include the effects of mechanical coupling. Experiment shows, however, that flexural modes in rectangular plates of quartz, tourmaline and nickel are often coupled with other modes of vibration.

This paper presents a two-dimensional theory of longitudinal and flexural vibrations in rectangular isotropic plates. This theory is more general than any known to the writers and includes the phenomenon of mechanical coupling. It is hoped that the following considerations will

[1] Giebe and Scheibe, Ann. d. Physik (5) **9**, 93, 137 (1931).
[2] H. Osterberg, Proc. Nat. Acad. Sci. **15**, 892 (1929).
[3] H. Osterberg, J. Opt. Soc. Am. **23**, 30 (1933).
[4] H. Osterberg, Phys. Rev. **43**, 819 (1933).
[5] H. Osterberg, Rev. Sci. Inst. **5**, 183 (1934).
[6] F. R. Lack, Proc. I. R. E. **17**, 1123 (1929).
[7] R. C. Hitchcock, Rev. Sci. Inst. **1**, 13 (1930).
[8] Rayleigh, *Theory of Sound*, Vol. 1, 1894, p. 255.
[9] S. P. Timoshenko, Phil. Mag. **41**, 744 (1921).
[10] S. P. Timoshenko, Phil. Mag. **43**, 125 (1922).
[11] H. Doerffler, Zeits. f. Physik **63**, 30 (1930).
[12] E. Goens, Ann. d. Physik (5) **11**, 649 (1931).

suggest methods by means of which the three-dimensional or general case can be solved to a degree of approximation suitable for the many experimental and practical purposes to which vibrating plates, both isotropic and anisotropic, have been applied.

Mechanical Coupling

When the dimensions and elastic properties of an elastic plate favor the mechanical coupling of two modes whose uncoupled or natural frequencies of vibration are n_1 and n_2, the displacements of these modes combine to form two vibrational patterns whose frequencies differ from n_1 and n_2. A knowledge of the manner in which the displacements of the uncoupled modes are combined to form the two vibrational patterns is essential to an understanding of the following theory.

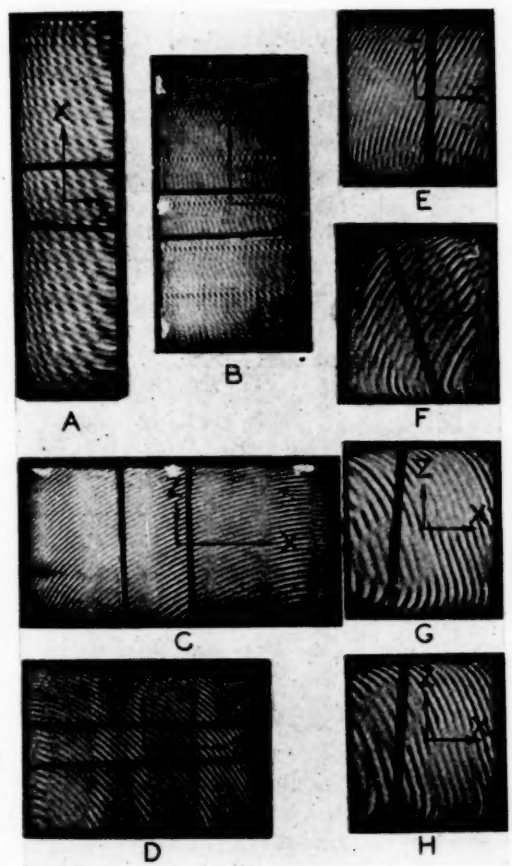

FIG. 1. Patterns illustrating the mechanical coupling of flexural modes. *A*, 415.6 kc/sec., crystal 1; *B*, 162.0 kc/sec., crystal 2; *C*, 34.65 kc/sec., crystal 2; *D*, 114.4 kc/sec., crystal 3; *E*, 100.1 kc/sec., crystal 4; *F*, 108.3 kc/sec., crystal 4; *G* and *H*, 205.5 kc/sec., crystal 4, *H* at the higher frequency.

Several nickel bars were placed in an alternating magnetic field and their vibrations examined in the simple interferometer. As in the case of quartz, these bars are in resonance at a large number of frequencies. Longitudinal, torsional and flexural modes are easily excited by applying the magnetic field along the length of the bar or plate. The vibrational patterns are in many respects similar to the corresponding patterns in quartz. The method of mechanical coupling is the same.

On account of the difficulties encountered in securing suitable photographs from the nickel bars, the method of coupling is here illustrated by means of the interference patterns of Fig. 1 which have been photographed from quartz plates 1, 2, 3 and 4 in the simple interferometer.[13] These patterns are examples of flexural modes of vibration.

The photographs of Fig. 1 reveal the arrangement of the nodes and antinodes of vibration of the Y faces (i.e., those perpendicular to Y) of the Y-cut plates listed in Table I. When the quartz plate is at rest, a set of thin film interference fringes are formed in the usual way between the Y face and an auxiliary piece of plate glass. (It is not necessary that the fringes should be straight.) When the plate is caused to vibrate, the thin film fringes are disturbed and blurred upon those portions of the Y face which enjoy a normal component of motion. On those portions whose normal component of motion is zero, the thin film fringes remain undisturbed. In the photographs the areas upon which the fringes are blurred (i.e., antinodal areas) stand out in sharp contrast to the areas upon which the fringes remain undisturbed (i.e., areas about

TABLE I. *Crystal quartz plates.*

Plate	Cut	x(mm)	y(mm)	z(mm)
1	Y	48.793	2.007	12.685
2	Y	47.65	5.673	24.76
3	Y	24.252	2.966	35.46
4	Y	15.969	7.123	18.124

[13] H. Osterberg, J. Opt. Soc. Am. **23**, 34 (1933).

the nodal lines). For further details concerning the interpretation of the fringe patterns the reader is referred to an earlier paper.[14]

In patterns A and B (Fig. 1) these nodes and antinodes are quite straight. This shows that the motion is due to the propagation of a very weakly coupled flexural wave train along X. As far as can be judged from the appearance of the Y faces, patterns A and B are examples of almost uncoupled flexural patterns. The antinodes of C show somewhat more curvature than those of A or B. In D the six antinodes are markedly curved. The displacements of this pattern are due to the mechanical coupling of the fourth flexural harmonic (the first flexural harmonic presents three antinodes) with another mode of vibration. The nature of this mode has not been determined.

Patterns E and F illustrate the two vibrational patterns which are formed by the mechanical coupling of the first harmonics of the two flexural modes in which the flexural wave trains are propagated along Z and X, respectively. The three antinodes of vibration of the Y faces in each of these harmonics are indicated by the shaded areas in Fig. 2. An antinode is marked with a plus sign when the instantaneous direction of motion of the surface is outward. Since the frequency of vibration of both sets of antinodes must be the same in a given coupled pattern, it follows that these sets of antinodes can be combined only in two different and distinct manners. Thus, for the indicated instantaneous motion of one set of antinodes, the motion of the other set of antinodes is that indicated either by P or by Q. In Fig. 1 F the relative phases of the coupled harmonics is that indicated by P; in Fig. 1 E their relative phases is that indicated by Q.

Further inspection of Fig. 1 E will show that the displacements of the wave train propagated along Z are greater than the displacements of the wave train propagated along X. In F, the displacements of the wave train propagated along X are the greater.

From the above examples, one may conclude that *two coupled modes m' and n' are formed by combining the displacements of the uncoupled modes m and n such that the displacements of m with respect to those of n in the case of m' are opposite in sign to the displacements of m with respect to n in the case of n'.*

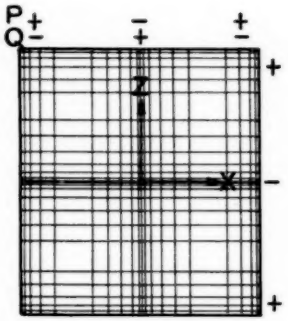

FIG. 2. Mechanical coupling of flexural modes.

The above conclusion applies also to the coupled modes of patterns G and H, which are formed by combining the second flexural harmonics in a manner similar to that in which the first harmonics are combined to form patterns E and F. As another illustration, the reader may refer to an earlier paper.[3] A study of several longitudinal patterns in quartz plates has in every case supported the above conclusion. A similar study of a large number of mixed patterns has shown that this is also the manner in which the displacements are combined in the coupling of both flexural and longitudinal modes with torsional modes of vibration.

The displacements of a given mode are represented in the following theory by the proper sinusoidal function. Physically, the displacements of a vibrational pattern which is formed by the mechanical coupling of two given modes are the sum of the displacements of these modes. Mathematically, the displacements of this vibrational pattern are the sum of the two sinusoidal functions which represent the separate displacements of the two modes. Let these functions be denoted by ϕ and ψ. The physical considerations of the previous paragraphs show that ϕ and ψ can be combined in only two different and distinct ways. These are $M'=\phi+\psi$ and $N'=\phi-\psi$. Further, these considerations also show that M' and N' represent the displacements of the two vibrational patterns formed by the mechanical coupling of the two individual modes.

It is not true physically that any two modes

[14] H. Osterberg, J. Opt. Soc. Am. **22**, 21 (1932).

possess the property of intercoupling mechanically. Now, M' and N' must satisfy the differential equations of motion of the elastic solid and an appropriate set of boundary conditions. Whether M' and N' represent a mechanically coupled combination of ϕ and ψ or whether they represent merely the superposition of ϕ and ψ can be determined from the equations of motion and the boundary conditions.

Equations of Motion: Boundary Conditions

The frequency expressions are derived upon the simplifying assumption and approximation that the displacements u and v are independent of z and that the displacement $w=0$. The equations of motion of a free isotropic plate now become in the notation of Love[15]

$$\mu\left(\frac{\partial^2 u}{\partial^2 x}+\frac{\partial^2 u}{\partial^2 y}\right)+(\lambda+\mu)\frac{\partial}{\partial x}\left(\frac{\partial u}{\partial x}+\frac{\partial v}{\partial y}\right)=\rho\frac{\partial^2 u}{\partial^2 t};$$
$$\mu\left(\frac{\partial^2 v}{\partial^2 x}+\frac{\partial^2 v}{\partial^2 y}\right)+(\lambda+\mu)\frac{\partial}{\partial y}\left(\frac{\partial u}{\partial x}+\frac{\partial v}{\partial y}\right)=\rho\frac{\partial^2 v}{\partial^2 t}. \qquad (1)$$

Let the origin of the Cartesian coordinates be located at the center of the rectangular parallelepiped whose x, y and z dimensions are respectively $2x'$, $2y'$ and $2z'$. The parallelepiped is so oriented that its three perpendicular edges are parallel to X, Y and Z. The boundary conditions, to which the solutions of (1) are to be subjected, are the statements that the surfaces of the parallelepiped are free or that the normal components of surface traction across these surfaces are zero at every point. These statements may be derived from (2). They are equivalent to (3).

$$X_\nu=X_x\cos(x\nu)+X_y\cos(y\nu)+X_z\cos(z\nu),$$
$$Y_\nu=Y_x\cos(x\nu)+Y_y\cos(y\nu)+Y_z\cos(z\nu), \qquad (2)[16]$$
$$Z_\nu=Z_x\cos(x\nu)+Z_y\cos(y\nu)+Z_z\cos(z\nu).$$

$X_x=0$ when $x=\pm x'$;

$Y_y=0$ when $y=\pm y'$;

$Z_z=0$ when $z=\pm z'$;

$X_x=Y_y=X_y=0$ when $x=\pm x'$ and $y=\pm y'$;
$Y_y=Z_z=Y_z=0$ when $y=\pm y'$ and $z=\pm z'$;
$X_x=Z_z=Z_x=0$ when $x=\pm x'$ and $z=\pm z'$;
$X_x=Y_y=Z_z=Y_z=Z_z=X_y=0$, when
$x=\pm x'$, $y=\pm y'$, $z=\pm z'$. (3)

From the above assumption regarding u, v and w the stress components in this two-dimensional case are independent of z. Hence (3) reduces to

$X_x=Z_x=Z_z=0$ when $x=\pm x'$;
$Y_y=Y_z=Z_z=0$ when $y=\pm y'$;
$X_y=0$ when $x=\pm x'$ and $y=\pm y'$. (4)

$$Z_z[17]=(\lambda+2\mu)\frac{\partial w}{\partial z}+\lambda\left(\frac{\partial u}{\partial x}+\frac{\partial v}{\partial y}\right)=\lambda\left(\frac{\partial u}{\partial x}+\frac{\partial v}{\partial y}\right).$$

It follows that $Z_z\neq 0$ unless $\lambda=0$ or $\partial u/\partial x+\partial v/\partial y=0$. Neither of the latter is in general true. The failure to satisfy the condition on Z_z is inherent in the approximations involved in the simplifying assumptions. Fortunately, λ is small as compared to $\lambda+2\mu$.

In the solutions presented by Madelung and Timoshenko no direct attempt is made to satisfy the condition upon X_x. The following solutions satisfy (3) with the single exception of the condition on Z_z.

The Longitudinal Case

A solution of the longitudinal type

$$u=a\sin\alpha x\cosh my\sin\omega t;$$
$$v=b\cos\alpha x\sinh my\sin\omega t \qquad (5)$$

will be found to satisfy (1) provided

$$\mu(m^2-\alpha^2)u-(\lambda+\mu)(\alpha/a)(a\alpha+bm)u+\rho\omega^2=0,$$
$$\mu(m^2-\alpha^2)v+(\lambda+\mu)(m/b)(a\alpha+bm)v+\rho\omega^2 v=0. \qquad (6)$$

Following Madelung,[11] (6) is satisfied by two values of b such that

[15] Love, *The Mathematical Theory of Elasticity*, 1927, p. 293.

[16] Reference 15, p. 78.

[17] Reference 15, p. 102.

$$b_1=-m_1a_1/\alpha; \quad b_2=-\alpha a_2/m_2. \tag{7}$$

This gives rise to two solutions of the form (5) and whose sum is a more general solution. This solution will be called a characteristic solution. It may be written

$$u=(M\cosh my+N\cosh ny)\sin\alpha x\sin\omega t,$$
$$v=-((Mm/\alpha)\sinh my+(N\alpha/n)\sinh ny)\cos\alpha x\sin\omega t. \tag{8}$$

From (6) and (7) the conditions upon m and n are seen to be

$$\rho\omega^2+(\lambda+2\mu)(m^2-\alpha^2)=0, \quad \rho\omega^2+\mu(n^2-\alpha^2)=0. \tag{9}$$

The characteristic solution (8) represents any odd harmonic of the standing longitudinal wave train whose direction of propagation is X. For brevity, let the corresponding mode of vibration be denoted as the longitudinal X mode. The motions of the surfaces AB, BC, CD and DA in the case of the first harmonic of the longitudinal X mode are indicated by the full arrows in Fig. 3. These motions are analogous to those of an open ended organ pipe whose walls are constructed of an elastic material such as rubber. The X faces AB and CD vibrate quite uniformly. Hence u may be described as a slow function of y. The Y faces vibrate such that $v=0$ when $x=\pm x'$ and such that v is a maximum when $x=0$. Note, also, that $u=0$ when $x=0$ and that $v=0$ when $y=0$. In the nth odd harmonic the Y faces possess n antinodes of vibration. Again, $v=0$ when $x=\pm x'$, v is a maximum when $x=0$, $v=0$ when $y=0$, $u=0$ when $x=0$, and u is a maximum when $x=\pm x'$. In view of these observations, it is natural to select (8) to represent any odd harmonic of the longitudinal X mode. The number of the harmonic enters into the choice of α.

In a similar manner, a solution of the type

$$u=a\cos\alpha x\cosh my\sin\omega t; \quad v=-b\sin\alpha x\sinh my\sin\omega t \tag{10}$$

may be substituted into (1) and shown to result in a characteristic solution of the form

$$u=(M\cosh my+N\cosh ny)\cos\alpha x\sin\omega t,$$
$$v=((Mm/\alpha)\sinh my+(N\alpha/n)\sinh ny)\times\sin\alpha x\sin\omega t, \tag{11}$$

in which m and n are again subject to (9). This characteristic solution represents an even harmonic of the standing longitudinal wave train whose direction of propagation is X. This may be seen by studying the motions of AB, BC, CD and DA in the case of the second harmonic described in Fig. 4.

A longitudinal solution of the form

$$u=-a\sin\beta y\sinh lx\sin\omega t; \quad v=b\cos\beta y\cosh lx\sin\omega t \tag{12}$$

satisfies (1) provided

$$\mu(l^2-\beta^2)u+(\lambda+\mu)(l/a)(al+b\beta)u+\rho\omega^2u=0,$$
$$\mu(l^2-\beta^2)v-(\lambda+\mu)(\beta/b)(al+b\beta)v+\rho\omega^2v=0. \tag{13}$$

$$\text{Let} \quad a_1=-b_1l_1/\beta \quad \text{and} \quad a_2=-b_2\beta/l_2. \tag{14}$$

As in (7) and (8), the characteristic solution may be written

$$u=((Kk/\beta)\sinh kx+(L\beta/l)\sinh lx)\sin\beta y\sin\omega t,$$
$$v=(K\cosh kx+L\cosh lx)\cos\beta y\sin\omega t \tag{15}$$

in which k and l are subject to

$$\rho\omega^2+(\lambda+2\mu)(k^2-\beta^2)=0, \quad \rho\omega^2+\mu(l^2-\beta^2)=0. \tag{16}$$

The characteristic solution (15) represents a longitudinal wave train whose direction of propagation is Y. It is an even harmonic of the longitudinal Y mode.

Similarly, a solution of the form

$$u=a\cos\beta y\sinh lx\sin\omega t; \quad v=b\sin\beta y\cosh lx\sin\omega t \tag{17}$$

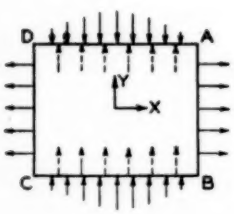

FIG. 3.

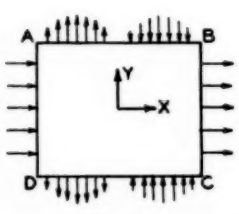

FIG. 4.

Mechanical coupling of longitudinal modes.

results in a characteristic solution of the type

$$u=-((Kk/\beta)\sinh kx + (L\beta/l)\sinh lx)\cos\beta y\sin\omega t,$$
$$v=(K\cosh kx+L\cosh lx)\sin\beta y\sin\omega t, \qquad (18)$$

in which k and l are subject to (16). This solution may be interpreted as an odd harmonic of the longitudinal Y mode.

An inspection of (8), (11), (15) and (18) shows that u and v assume the form $F(x)G(y)\sin\omega t$ where F and G are sinusoidal or hyperbolic. It will be found that (1) is satisfied only when certain F's and G's are selected. The various possible combinations for u and v are the characteristic solutions and these may be grouped into the longitudinal, flexural or other types from the displacements which they describe. In these considerations the characteristic solutions are limited to those which may be interpreted as longitudinal wave trains propagated along X or Y. Within this limitation, the most general solution consists of a linear combination of the possible characteristic solutions.

This more general solution is most easily studied by considering some of its simpler linear combinations. The resulting frequency expressions are of immediate experimental importance.

Consider the combination which gives rise to the more complicated frequency expression. From (8) and (18) one forms the linear combination[18]

$$u_1=[(M\cosh my+N\cosh ny)\sin\alpha x-((Kk/\beta)\sinh kx+(L\beta/l)\sinh lx)\cos\beta y]\sin\omega t,$$
$$v_1=[-((Mm/\alpha)\sinh my+(N\alpha/n)\sinh ny)\cos\alpha x+(K\cosh kx+L\cosh lx)\sin\beta y]\sin\omega t. \qquad (19)$$

This and following combinations satisfy the conditions on Y_z and Z_x since from the assumptions on u, v and w

$$Y_z^{17}=\mu(\partial v/\partial z+\partial w/\partial y)=0;\quad Z_x^{17}=\mu(\partial u/\partial z+\partial w/\partial x)=0. \qquad (20)$$

From (4)
$$x_x^{17}=(\lambda+2\mu)\partial u/\partial x+\lambda\partial v/\partial y=0,\quad x=\pm x'. \qquad (21)$$

From (19) and (21)

$$0=(\lambda+2\mu)[\alpha(M\cosh my+N\cosh ny)\cos\alpha x'-((Kk^2/\beta)\cosh kx'+L\beta\cosh lx')\cos\beta y]$$
$$-\lambda[((Mm^2/\alpha)\cosh my+N\alpha\cosh ny)\cos\alpha x'-\beta(K\cosh kx'+L\cosh lx')\cos\beta y]. \qquad (22)$$

This is satisfied for any value of y provided $\cos\alpha x'=0$ and

$$K[(\lambda+2\mu)k^2/\beta-\lambda\beta]\cosh kx'+2\mu\beta L\cosh lx'=0. \qquad (23)$$

From (4)
$$Y_y^{17}=(\lambda+2\mu)\partial v/\partial y+\lambda\partial u/\partial x=0,\quad y=\pm y'. \qquad (24)$$

From (19) and (24)

$$0=\lambda[\alpha(M\cosh my'+N\cosh ny')\cos\alpha x-((Kk^2/\beta)\cosh kx+L\beta\cosh lx)\cos\beta y']$$
$$-(\lambda+2\mu)[((Mm^2/\alpha)\cosh my'+N\alpha\cosh ny')\cos\alpha x-\beta(K\cosh kx+L\cosh lx)\cos\beta y']. \qquad (25)$$

This is satisfied for any value of x provided $\cos\beta y'=0$ and

$$M[(\lambda+2\mu)m^2/\alpha-\lambda\alpha]\cosh my'+2\mu\alpha N\cosh ny'=0. \qquad (26)$$

Finally,
$$X_y^{17}=\mu(\partial v/\partial x+\partial u/\partial y)=0 \quad \text{when} \quad x=\pm x',\quad y=\pm y'. \qquad (27)$$

From (19) and (27)

$$0=(Mm\sinh my'+Nn\sinh ny')\sin\alpha x'+\beta((kK/\beta)\sinh kx'+(L\beta/l)\sinh lx')\sin\beta y'$$
$$+\alpha((Mm/\alpha)\sinh my'+(N\alpha/n)\sinh ny')\sin\alpha x'+(Kk\sinh kx'+Ll\sinh lx')\sin\beta y'. \qquad (28)$$

[18] The linear combinations here considered satisfy the conditions of compatibility.

But $\pm \sin \alpha x' = \sin \beta y' = \pm 1$; hence

$$0 = (2mM \sinh my' + ((n^2+\alpha^2)/n)N \sinh ny') \pm (2kK \sinh kx' + ((\beta^2+l^2)/l)L \sinh lx'), \quad (29)$$

in which the positive sign is chosen when $\sin \alpha x'$ and $\sin \beta y'$ are of the same sign.

Since the actual amplitude of oscillation is not desired, no loss in generality is suffered by setting

$$N = L = 1. \quad (30)$$

From (9), (16), (23), (26), (29) and (30) one forms the frequency expression

$$0 = \sinh ny' \left[\frac{2m}{1-\rho\omega^2/2\mu\alpha^2} \frac{\tanh my'}{\tanh ny'} - \frac{n^2+\alpha^2}{n} \right] \pm \sinh lx' \left[\frac{2k}{1-\rho\omega^2/2\mu\beta^2} \frac{\tanh kx'}{\tanh lx'} - \frac{\beta^2+l^2}{l} \right], \quad (31)$$

in which the positive sign is chosen when $\sin \alpha x'$ and $\sin \beta y'$ are alike in sign. k, l, m and n are easily eliminated from (31) by means of (9) and (16). The expression so obtained relates ω to x', y', λ and μ since α and β are known from (23) and (26). The frequency of vibration ($f = \omega/2\pi$) is thus known theoretically.

Since $\cos \alpha x' = \cos \beta y' = 0$,

$$\alpha = p\pi/2x', \; p = 1, 3, 5, \text{ etc.} \quad \text{and} \quad \beta = q\pi/2y', \; q = 1, 3, 5, \text{ etc.} \quad (32)$$

A similar linear combination is obtained by reversing the signs of the last terms in u_1 and v_1. Thus

$$\begin{aligned} u_2 &= [(M \cosh my + N \cosh ny) \sin \alpha x + ((Kk/\beta) \sinh kx + (L\beta/l) \sinh lx) \cos \beta y] \sin \omega t, \\ v_2 &= [-((Mm/\alpha) \sinh my + N\alpha/n \sinh ny) \cos \alpha x - (K \cosh kx + L \cosh lx) \sin \beta y] \sin \omega t. \end{aligned} \quad (33)$$

When (33) is subjected to the boundary conditions in the manner illustrated in the case of (19), the following frequency expression is obtained:

$$0 = \sinh ny' \left[\frac{2m}{1-\rho\omega^2/2\mu\alpha^2} \frac{\tanh my'}{\tanh ny'} - \frac{n^2+\alpha^2}{n} \right] \mp \sinh lx' \left[\frac{2k}{1-\rho\omega^2/2\mu\beta^2} \frac{\tanh kx'}{\tanh lx'} - \frac{\beta^2+l^2}{l} \right], \quad (34)$$

in which the negative sign is selected when $\sin \alpha x'$ and $\sin \beta y'$ are of like sign. It is also found that (32) must be satisfied. A comparison of (31) and (34) shows that for a given value of α and β they differ only in the sign of the last member.

In solutions (19) and (33) the first and second terms represent the odd harmonics of longitudinal X and Y modes. It will be noted that the relative displacements of the X and Y waves in (19) are opposite in sign to the relative displacement of these waves in (33). Solutions (19) and (33) therefore describe the displacements of the two coupled modes formed by combining these X and Y modes. This follows from the statements found at the end of the preceding section on mechanical coupling by identifying (8) with ϕ and (18) with ψ and noting the manner in which ϕ and ψ enter (19) and (33). The frequencies of the coupled modes are predicted by Eqs. (31) and (34). Any set of odd harmonics of the X and Y modes may be coupled, depending upon which p and q are chosen in accordance with (32).

It has therefore been shown that a linear combination of the odd harmonics of the X and Y modes forms a mechanically coupled system.

It will next be shown that a linear combination of an even harmonic of the X mode with an odd harmonic of the Y mode, an odd harmonic of the X mode with an even harmonic of the Y mode, or an even harmonic of the X mode with an even harmonic of the Y mode does not form a mechanically coupled combination. Such modes are, within the limitations of this theory, mutually independent.

Consider a linear combination of the even harmonics of the X and Y modes. Combining (11) and (15),

$$u_3=[(M\cosh my+N\cosh ny)\cos\alpha x+((Kk/\beta)\sinh kx+(L\beta/l)\sinh lx)\sin\beta y]\sin\omega t,$$
$$v_3=[((Mm/\alpha)\sinh my+(N\alpha/n)\sinh ny)\sin\alpha x+(K\cosh kx+L\cosh lx)\cos\beta y]\sin\omega t. \quad (35)$$

From (21) and (35) one obtains

$$\sin\alpha x'=0, \quad \text{and} \quad 2\mu\beta L\cosh lx'+K[(\lambda+2\mu)k^2/\beta-\lambda\beta]\cosh kx'=0. \quad (36)$$

From (24) and (35)

$$\sin\beta y'=0, \quad \text{and} \quad 2\mu\alpha N\cosh ny'+M[(\lambda+2\mu)m^2/\alpha-\lambda\alpha]\cosh my'=0. \quad (37)$$

From (27) and (35),

$$0=(Mm\sinh my+Nn\sinh ny)\cos\alpha x+\beta((Kk/\beta)\sinh kx+(L\beta/l)\sinh lx)\cos\beta y$$
$$+\alpha((Mm/\alpha)\sinh my+(N\alpha/n)\sinh ny)\cos\alpha x+(Kk\sinh kx+Ll\sinh lx)\cos\beta y. \quad (38)$$

This equation should be contrasted with (28). Since it must hold for $x=\pm x'$ and $y=\pm y'$, it is necessary that

$$2kK\sinh kx'+[(l^2+\beta^2)/l]L\sinh lx'=0; \quad 2mM\sinh my'+[(n^2+\alpha^2)/n]N\sinh ny'=0. \quad (39)$$

Whereas (28) is satisfied by one condition (29), two independent conditions (39) are required to satisfy (38).

When K, L, M and N are eliminated by combining (36), (37) and (39), the frequency expressions are seen to be two in number and assume the forms

$$\frac{\tanh kx'}{\tanh lx'}=\frac{l^2+\beta^2}{4\mu kl\beta}\left[(\lambda+2\mu)\frac{k^2}{\beta}-\lambda\beta\right]; \quad (40) \qquad \frac{\tanh my'}{\tanh ny'}=\frac{n^2+\alpha^2}{4\mu mn\alpha}\left[(\lambda+2\mu)\frac{m^2}{\alpha}-\lambda\alpha\right]. \quad (41)$$

k, l, m and n are easily eliminated by means of (9) and (16). α and β are known from (36) and (37). Thus,

$$\alpha=p'\pi/2x', \; p'=2, 4, 6, \text{etc.}; \quad \beta=q'\pi/2y', \; q'=2, 4, 6, \text{etc.} \quad (42)$$

Eq. (41) determines the frequency of the X mode while (40) determines that of the Y mode. Since (40) and (41) are independent, it follows that the even harmonics of these modes do not form a coupled system.

Eqs. (40) and (41) give the dependence of the frequency of the X and Y modes upon the x and y dimensions. They include the "Rayleigh correction" since they take into account the kinetic energy involved in both of the displacements u and v.

When an even harmonic of the X mode is combined with an odd harmonic of the Y mode and this linear combination is considered in a manner similar to (35), it is found that

$$\alpha=p'\pi/2x', \; p'=2, 4, 6, \text{etc.}; \quad \beta=q\pi/2y', \; q=1, 3, 5, \text{etc.} \quad (43)$$

and that frequency expressions are identically (40) and (41). When an odd harmonic of the X mode and an even harmonic of the Y mode are similarly considered, it is found that

$$\alpha=p\pi/2x', \; p=1, 3, 5, \text{etc.}; \quad \beta=q'\pi/2y', \; q'=2, 4, 6, \text{etc.} \quad (43a)$$

and that (40) and (41) again hold.

It has therefore been shown that *the linear combinations of the longitudinal X and Y modes which form a mechanically coupled system are only those which consist of the odd harmonics of both of these modes.*

The most general solution may now be considered. It consists of a linear combination of every possible characteristic solution. Most of these, however, are independent of one another and give rise to frequencies of vibration which may be computed from (40) or (41) together with (42), (43) and (44). Any particular odd harmonic of the X mode is coupled with every odd harmonic of the Y mode, and *vice versa*. This may be stated as follows: "A mechanically coupled system is associated with every odd harmonic of either the X or Y mode." An infinite number of frequencies is theoretically associated with each coupled system provided an infinite number of overtones is possible.

Consider, briefly, the mechanically coupled system in which the pth odd harmonic of the X mode is coupled with the first s odd harmonics of the Y mode. The displacements u and v may be written

$$u=\left[(M_p\cosh m_p y+N_p\cosh n_p y)\sin\alpha_p x+\sum_{r=1}^{r=s}\mp\left(\frac{K_r k_r}{\beta_r}\sinh k_r x+\frac{L_r\beta_r}{l_r}\sinh l_r x\right)\cos\beta_r y\right]\sin\omega t;$$

$$v=\left[-\left(\frac{M_p m_p}{\alpha_p}\sinh m_p y+\frac{N_p\alpha_p}{n_p}\sinh n_p y\right)\cos\alpha_p x+\sum_{r=1}^{r=s}\pm(K_r\cosh k_r x+L_r\cosh l_r x)\sin\beta_r y\right]\sin\omega t. \tag{44}$$

When (44) is substituted into (21), (24) and (27), a number of frequencies of vibration is obtained. The number of frequencies is equal to the number of different and distinct ways in which the s odd harmonics can be combined with the X mode by choosing the plus or minus sign before the individual harmonics as in (44). As an example of one of these frequencies, that obtained by choosing the positive sign throughout is given by

$$0=\left[\frac{2m_p}{1-\rho\omega^2/2\mu\alpha_p^2}\frac{\tanh m_p y'}{\tanh n_p y'}-\frac{n_p^2+\alpha_p^2}{n_p}\right]\sinh n_p y'$$
$$+\sum_{r=1}^{r=s}\left[\frac{2k_r}{1-\rho\omega^2/2\mu\beta_r^2}\frac{\tanh k_r x'}{\tanh l_r x'}-\frac{\beta_r^2+l_r^2}{l_r}\right]\sinh l_r x', \tag{45}$$

where $\alpha_p=p\pi/2x'$; $\beta_r=r\pi/2y'$; p and r are odd and so chosen that $\sin\alpha_p x'$ and $\sin\beta_r y'$ are of like sign. When the positive sign is not chosen throughout, a negative sign precedes those members within the summation of (45) which are associated with the second choice of sign in (44).

It is to be expected that the most important terms in the summation of (45) are those for which α_p is the most nearly equal to β_r. A good approximation should be obtained by considering only the nearest or the two nearest harmonics in this respect.

The conclusion that only the odd harmonics of the two modes are capable of forming a coupled system was at first surprising. The following considerations, which may be carried further by the reader, show that this conclusion is physically reasonable. The first harmonic of the X mode (Fig. 3) causes the surfaces AB, BC, CD and AD to move as indicated by the arrows. It is easily seen that the motions of BC and AD are capable of exciting (and thus coupling with) any odd harmonic of the Y mode since for the odd harmonics AD and BC enjoy the same type of relative motion as do AB and CD. The motions of AD and BC are not, however, capable of inducing the even harmonics of the Y mode since these give rise to relative motions of AD and CB of the type indicated by the broken arrows. The even harmonics of the X mode cause AB, BC, CD and AD to vibrate as indicated in Fig. 3. The motions of AB and CD are not capable of inducing either the even or the odd harmonics of the Y mode.

The above coupling phenomenon was beautifully demonstrated by means of a square quartz plate of Z cut. In this plate the first harmonics of the X and Y mode were closely coupled, as were also the third harmonics, but the second harmonics appeared to be uncoupled. This phenomenon was most easily observed in the refracting[5] interferometer or by placing the plate between nicol prisms.

The Flexural Case

The assumptions are again made that u and v are independent of z and that $w=0$. The solutions for this case are in many respects similar to those of the longitudinal case. On this account and for the sake of brevity the results for the flexural case are presented in less detail.

The possible characteristic solutions are obtained as in the longitudinal case. They are as follows:

$$\begin{aligned} u &= (M \sinh my + N \sinh ny) \cos \alpha x \sin \omega t, \\ v &= ((Mm/\alpha) \cosh my + (N\alpha/n) \cosh ny) \sin \alpha x \sin \omega t, \end{aligned} \tag{46}$$

$$\begin{aligned} u &= (M \sinh my + N \sinh ny) \sin \alpha x \sin \omega t, \\ v &= -((Mm/\alpha) \cosh my + (N\alpha/n) \cosh ny) \cos \alpha x \sin \omega t, \end{aligned} \tag{47}$$

$$\rho\omega^2 + (\lambda+2\mu)(m^2-\alpha^2) = 0; \quad \rho\omega^2 + \mu(n^2-\alpha^2) = 0. \tag{48}$$

The symbols do not necessarily correspond to those of the longitudinal case. Since the two cases are considered separately, these symbols may be used again without introducing ambiguity.

Eq. (46) represents an even harmonic of the flexural X mode, i.e., of that mode due to the propagation of standing flexural wave trains along X. Eq. (47) describes an odd harmonic.

The remaining characteristic solutions represent the even and odd harmonics of the flexural Y mode. They are, respectively:

$$\begin{aligned} u &= ((Kk/\beta) \cosh kx + (L\beta/l) \cosh lx) \sin \beta y \sin \omega t, \\ v &= (K \sinh kx + L \sinh lx) \cos \beta y \sin \omega t; \end{aligned} \tag{49}$$

$$\begin{aligned} u &= -((Kk/\beta) \cosh kx + (L\beta/l) \cosh lx) \cos \beta y \sin \omega t, \\ v &= (K \sinh kx + L \sinh lx) \sin \beta y \sin \omega t. \end{aligned} \tag{50}$$

$$\rho\omega^2 + (\lambda+2\mu)(k^2-\beta^2) = 0, \quad \rho\omega^2 + \mu(l^2-\beta^2) = 0. \tag{51}$$

A linear combination of the characteristic solutions for the even harmonics of the X and Y modes may be written

$$\begin{aligned} u_1 &= [(M \sinh my + N \sinh ny) \cos \alpha x \pm ((Kk/\beta) \cosh kx + (L\beta/l) \cosh lx) \sin \beta y] \sin \omega t, \\ v_1 &= [((Mm/\alpha) \cosh my + (N\alpha/n) \cosh ny) \sin \alpha x \pm (K \sinh kx + L \sinh lx) \cos \beta y] \sin \omega t. \end{aligned} \tag{52}$$

When (52) is substituted into (21), (24) and (27) and the equations so obtained used to eliminate K and M (setting as before $N=L=1$), the frequency expression assumes the form,

$$0 = \cosh ny' \left[\frac{2m}{1-\rho\omega^2/2\mu\alpha^2} \frac{\tanh ny'}{\tanh my'} - \frac{n^2+\alpha^2}{n} \right] \pm \cosh lx' \left[\frac{2k}{1-\rho\omega^2/2\mu\beta^2} \frac{\tanh lx'}{\tanh kx'} - \frac{\beta^2+l^2}{l} \right], \tag{53}$$

in which $\cos \alpha x' = \cos \beta y' = \pm 1$. If α and β are so related that $\cos \alpha x' = -\cos \beta y' = \pm 1$, the corresponding frequency expression is obtained by choosing $\mp$ instead of $\pm$ in (53).

$$\alpha = p'\pi/2x', \; p' = 2, 4, 6, \text{ etc.}; \quad \beta = q'\pi/2y', \; q' = 2, 4, 6, \text{ etc.} \tag{54}$$

(53) shows that a linear combination of an even harmonic of the flexural X mode with an even harmonic of the flexural Y mode forms a mechanically coupled combination. An extension of the above argument will show that each even harmonic of the flexural X mode combines with every even harmonic of the Y mode to form a mechanically coupled system.

Consider the linear combinations

$$\begin{aligned} u_2 &= [(M \sinh my + N \sinh ny) \sin \alpha x \pm ((Kk/\beta) \cosh kx + (L\beta/l) \cosh lx) \sin \beta y] \sin \omega t, \\ v_2 &= [-((Mm/\alpha) \cosh my + (N\alpha/n) \cosh ny) \cos \alpha x \pm (K \sinh kx + L \sinh lx) \cos \beta y] \sin \omega t. \end{aligned} \tag{55}$$

Substituting (55) into (21), (24) and (27) and eliminating K, L, M and N,

$$\tanh lx'/\tanh kx' = [(l^2+\beta^2)/4\mu\beta kl][(\lambda+2\mu)(k^2/\beta)-\lambda\beta]; \tag{56}$$

$$\tanh ny'/\tanh my' = [(n^2+\alpha^2)/4\mu mn\alpha][(\lambda+2\mu)m^2/\alpha-\lambda\alpha]; \tag{57}$$

$$\cos \alpha x' = \sin \beta y' = 0 \quad \text{or} \quad \alpha = p\pi/2x',\ p=1,\ 3,\ 5,\ \text{etc.};\quad \beta = q'\pi/2y',\ q'=2,\ 4,\ 6,\ \text{etc.} \tag{58}$$

(55) consists of the sum of an odd harmonic of the X mode and an even harmonic of the Y mode. Since (56) and (57) are independent, these harmonics do not form a coupled combination.

Consider the linear combinations

$$\begin{aligned} u_3 &= [(M \sinh my + N \sinh ny) \cos \alpha x \mp ((Kk/\beta) \cosh kx + (L\beta/l) \cosh lx) \cos \beta y] \sin \omega t, \\ v_3 &= [((Mm/\alpha) \cosh my + (N\alpha/n) \cosh ny) \sin \alpha x \pm (K \sinh kx + L \sinh lx) \sin \beta y] \sin \omega t. \end{aligned} \tag{59}$$

These give rise to the frequency expressions (56) and (57) together with the conditions

$$\sin \alpha x' = \cos \beta y' = 0 \quad \text{or} \quad \alpha = p'\pi/2x',\ p'=2,\ 4,\ 6,\ \text{etc.};\quad \beta = q\pi/2y',\ q=1,\ 3,\ 5,\ \text{etc.} \tag{60}$$

An even harmonic of the flexural X mode and an odd harmonic of the Y mode do not, therefore, form a mechanically coupled combination.

Consider finally the combination

$$\begin{aligned} u_4 &= [(M \sinh my + N \sinh ny) \sin \alpha x \mp ((Kk/\beta) \cosh kx + (L\beta/l) \cosh lx) \cos \beta y] \sin \omega t, \\ v_4 &= [-((Mm/\alpha) \cosh my + (N\alpha/n) \cosh ny) \cos \alpha x \pm (K \sinh kx + L \sinh lx) \sin \beta y] \sin \omega t. \end{aligned} \tag{61}$$

(61) gives rise to the frequency expressions (56) and (57) together with

$$\cos \alpha x' = \cos \beta y' = 0 \quad \text{or} \quad \alpha = p\pi/2x',\ p=1,\ 3,\ 5,\ \text{etc.};\quad \beta = q\pi/2y',\ q=1,\ 3,\ 5,\ \text{etc.} \tag{62}$$

(61) combines an odd harmonic from each of the two modes. Consequently such harmonics do not form a coupled combination. It has therefore been shown that *in the flexural case the linear combinations of the X and Y modes which form a mechanically coupled system are only those which consist of the even harmonics of both of these modes.*

As in the longitudinal case, the most general solution consists of the sum of every possible characteristic solution. Most of these are independent and satisfy the frequency expressions (56) and (57). A mechanically coupled system is associated with every even harmonic of the X and Y modes. The displacements of the coupled system in which the jth even harmonic of the X mode is coupled with the first s even harmonics of the Y mode are

$$\begin{aligned} u &= \left[(M_j \sinh m_j y + N_j \sinh n_j y) \cos \alpha_j x + \sum_{r=2}^{r=s} \pm \left(\frac{K_r k_r}{\beta_r} \cosh k_r x + \frac{L_r \beta_r}{l_r} \cosh l_r x \right) \sin \beta_r y \right] \sin \omega t, \\ v &= \left[\left(\frac{M_j m_j}{\alpha_j} \cosh m_j y + \frac{N_j \alpha_j}{n_j} \cosh n_j y \right) \sin \alpha_j x + \sum_{r=2}^{r=s} \pm (K_r \sin k_r x + L_r \sinh l_r x) \cos \beta_r y \right] \sin \omega t. \end{aligned} \tag{63}$$

Comments similar to those made following (44) apply also to (63). As an example, the frequency expression obtained by choosing the negative sign throughout is

$$0 = \cosh n_j y' \left[\frac{2m_j}{1-\rho\omega^2/2\mu\alpha_j^2} \frac{\tanh n_j y'}{\tanh m_j y'} - \frac{n_j^2+\alpha_j^2}{n_j} \right] - \sum_{r=2}^{r=s} \cosh l_r x' \left[\frac{2k_r}{1-\rho\omega^2/2\mu\beta_r^2} \frac{\tanh l_r x'}{\tanh k_r x'} - \frac{l_r^2+\beta_r^2}{l_r} \right], \tag{64}$$

in which $\cos \alpha_j x' = \cos \beta_r y' = \pm 1$.

$$\alpha_j = j\pi/2x',\ j=2,\ 4,\ 6,\ \text{etc.};\quad \beta_r = r\pi/2y',\ r=2,\ 4,\ 6,\ \text{etc.} \tag{65}$$

The most important terms of (64) are those for which α_j is most nearly equal to β_r. The remainder of the terms may be neglected.

The conclusion that only an even harmonic of the two flexural modes is capable of forming a coupled system may perhaps seem even more surprising than the conclusion that only an odd harmonic of the two longitudinal modes enters into a mechanically coupled system. The relative motions of the surfaces of a rectangular plate which is vibrating flexurally have been determined by the writers. These motions are such as to confirm the above conclusion. Experiments determining the relative motions of the surfaces of a plate which is vibrating longitudinally and flexurally provide excellent evidence for the qualitative correctness of this theory.[19]

When m and n are eliminated from (57) by means of (48), the resulting frequency expression can be transformed directly into the expression studied by Doerffler.[20] His frequency measurements agree in general within two percent with the computed values. The experimental method employed by Doerffler is not well adapted for differentiating the more closely coupled flexural patterns from the more weakly coupled ones. Doerffler worked with quartz, but it will be shown elsewhere that this theory is applicable with good approximation to X and Y cuts of quartz.

An inspection of the displacements of (55), for example, will show that even when the displacements are due largely to the flexural X mode a definite contribution is made by the terms belonging to the Y mode. The form of the Y wave is of the type which is qualitatively correct for explaining the measured, systematic end correction or the inequalities in the distances between the nodes of a quartz plate vibrating flexurally. As will be seen from Fig. 1B, these nodal distances can be measured accurately. These will be considered elsewhere.

[19] In this connection it will be noted that in the patterns of Fig. 1 E and F the first odd harmonics of the flexural X and Y modes are closely coupled. The major displacements of this X mode, are, however, u and w while those of the Y mode are v and w. A pattern formed by combining the flexural X and Y modes which bend the plate in this manner does not belong to the two-dimensional case.

[20] H. Doerffler, Zeits. f. Physik **63**, 48 (1930).

The Velocity of Compressional Waves in a Rectangular Plate

The velocity of compressional waves in an infinite medium is well known[21] to be

$$v=\omega/\alpha=((\lambda+2\mu)/\rho)^{\frac{1}{2}}, \qquad \alpha=2\pi/L, \quad (66)$$

where L is the wavelength. This formula may be expected to approximate the formulae for the velocity of sound in a plate of finite dimensions. The velocity of compressional waves along a thin rod is approximated[22] by the expression

$$v=(E/\rho)^{\frac{1}{2}} \text{ where } E=\mu(3\lambda+2\mu)/(\lambda+\mu). \quad (67)[23]$$

A comparison of (66) and (67) shows that the calculated values of v approach each other only when λ is small as compared to μ.

Eq. (41) may be written

$$\frac{\tanh\left[\alpha y'(1-\rho\omega^2/\alpha^2(\lambda+2\mu))\right]}{\tanh\left[\alpha y'(1-\rho\omega^2/\mu\alpha^2)\right]} = \frac{(1-\rho\omega^2/2\mu\alpha^2)^2}{\left[(1-\rho\omega^2/\mu\alpha^2)(1-\rho\omega^2/\alpha^2(\lambda+2\mu))\right]^{\frac{1}{2}}}. \quad (68)$$

If $\lambda=0$, Eq. (68) is satisfied by such a value of ω that

$$1-\rho\omega^2/2\mu\alpha^2=0, \quad \text{or} \quad \omega^2/\alpha^2=v^2=2\mu/\rho. \quad (69)$$

Hence, (66), (67) and (68) agree when $\lambda=0$. When $\lambda\neq 0$, the value of v computed from (68) will not, in general, agree with that given either by (66) or (67). The velocity computed from (68) depends upon the x and y dimensions and the frequency of vibration. The limiting value of v at high frequency is obtained by equating the right-hand member of (68) to unity. A similar limiting value has been found by Timoshenko[24] for the velocity of flexural waves.

When the velocity of compressional waves is computed from the definition $v=\omega/\alpha$ or ω/β by using (31) or (34), it will be found that v departs considerably from its usual value for those values of p and q (Eq. (32)) for which α and β are nearly equal, i.e., the case in which the uncoupled frequencies of the two coupled modes are nearly alike. The velocity may be greater

[21] Reference 15, p. 302.
[22] Reference 21, p. 434.
[23] Reference 21, p. 101.
[24] S. P. Timoshenko, Phil. Mag. **43**, 128 (1922).

than or less than the usual value. This has frequently been confirmed at this laboratory.

The velocity of compressional waves in an isotropic plate is not a constant, as predicted from (67), but depends in a complicated manner upon a number of factors. Unfortunately, it also depends upon the viscosity of the vibrating medium.

The use of nickel bars, driven by an alternating magnetic field, for checking the quantitative aspects of the above theory involves the serious difficulty of controlling the temperature of the vibrating bar. The writers find that unless care is exercised this temperature may rise from room temperature to 200°C. On account of this difficulty the above theory of mechanical coupling will be checked by the use of oscillating quartz plates. It will be shown elsewhere that this theory applies also to vibrating quartz plates when it can be assumed that $w=0$ and that u and v are independent of z. It is necessary only to replace $\lambda+2\mu$ by the elastic constant c_{11} and μ by $(c_{11}-c_{12})/2$.

The writers wish to express their thanks to Professor H. W. March for his criticism of the manuscript and of the theory.

JULY, 1935 PHYSICS VOLUME 6

Longitudinal, Shear and Transverse Modes of Vibration in Quartz and Tourmaline

HAROLD OSTERBERG AND JOHN W. COOKSON, *Department of Physics, University of Wisconsin*

(Received July 18, 1934)

The general differential equations which describe the vibrations of plates of quartz or tourmaline are stated together with the corresponding boundary conditions for a free plate. Solutions are presented for the longitudinal modes in which pure compressional waves are propagated along *X*, *Y* or *Z* in quartz or tourmaline. Experiment shows that these modes are purest (i.e., their displacements most nearly limited to the direction of propagation) in rectangular plates whose greatest dimension is that along which the compressional wave trains are propagated. As this dimension is shortened, the longitudinal modes decrease in purity and finally fail to appear. The purest longitudinal mode in the usual *X*, *Y* or *Z* cuts of quartz is that in which compressional waves are propagated along *X* in *Y* or *Z* cuts. The vibrational patterns which correspond to the mode in which compressional waves are propagated along *Y* in *X* or *Z* cuts of quartz are so complicated that the correspondence is open to considerable doubt. These latter longitudinal modes were found in tourmaline, and appeared to be simpler than the corresponding modes in quartz. The elastic constants c_{11} and c_{33} were obtained with an experimental error of but 1/3 percent. These measurements differ by 3 to 7 percent from those made by Voigt. The simple shear, pure shear, transverse and the *yz*, *zx* and *xy* shear modes are defined and distinguished. The differential equations of motion are not satisfied by free periodic vibrations of the simple shear or the pure shear types. No experimental evidence was found for the existence of any type of free simple or pure shear modes in a large variety of *X*, *Y* and *Z* cuts of quartz. Whereas forced simple shear vibrations are theoretically possible in a *Y* cut, the free simple shear vibrations are not. Solutions are presented for the various types of transverse vibrations. Experimental evidence for these transverse vibrations was not obtained. More general theoretical considerations indicate that the free transverse modes do not exist. The *yz*, *zx* and *xy* shear modes were observed in suitably oriented *Y* cuts of α quartz. The observations upon the latter modes are compared with the observations of Mason and Lack, Willard and Fair. It is concluded that the mode which was employed by Lack, Willard and Fair was not a transverse mode, but rather, the *xy* shear mode. The predominant modes of vibration are of longitudinal, flexural or torsional nature. Crystals of β quartz are active oscillators even at 800°C and will be shown to be piezoelectric.

AMONG the descriptions[1-5] of various interference methods used at this laboratory for studying the vibrations of quartz plates are found brief and scattered remarks pertaining to the nature of the observed modes of vibration. Observations upon the modes of vibration in thin *X* or *Y* cuts are frequently in disagreement with those reported by others. Some of the more important facts which have been established as to the nature of the simpler modes are here

discussed. The flexural, the torsional and the complex longitudinal modes are not considered.

Equations of Motion: Boundary Conditions

It is well known that the equations of motion[6] for any elastic solid may be expanded by substituting into these equations the values of the components of stress in terms of the components of strain. In the absence of mechanical damping and of body forces, the expanded equations of motion for α quartz and tourmaline may be written in the notation of Love:

$$
\begin{aligned}
&c_{11}\frac{\partial^2 u}{\partial x^2}+\frac{c_{11}-c_{12}}{2}\frac{\partial^2 u}{\partial y^2}+c_{44}\frac{\partial^2 u}{\partial z^2}+2c_{14}\frac{\partial^2 u}{\partial y\partial z}+\frac{c_{11}+c_{12}}{2}\frac{\partial^2 v}{\partial x\partial y}+2c_{14}\frac{\partial^2 v}{\partial x\partial z}+2c_{14}\frac{\partial^2 w}{\partial x\partial y}\\
&\qquad+(c_{44}+c_{13})\frac{\partial^2 w}{\partial x\partial z}=\rho\frac{\partial^2 u}{\partial t^2};\\
&\frac{c_{11}-c_{12}}{2}\frac{\partial^2 v}{\partial x^2}+c_{11}\frac{\partial^2 v}{\partial y^2}+c_{44}\frac{\partial^2 v}{\partial z^2}+c_{14}\frac{\partial^2 w}{\partial x^2}-c_{14}\frac{\partial^2 w}{\partial y^2}+\frac{c_{11}+c_{12}}{2}\frac{\partial^2 u}{\partial x\partial y}+2c_{14}\frac{\partial^2 u}{\partial x\partial z}\\
&\qquad-2c_{14}\frac{\partial^2 v}{\partial y\partial z}+(c_{44}+c_{13})\frac{\partial^2 w}{\partial y\partial z}=\rho\frac{\partial^2 v}{\partial t^2};\\
&c_{44}\frac{\partial^2 w}{\partial x^2}+c_{44}\frac{\partial^2 w}{\partial y^2}+c_{33}\frac{\partial^2 w}{\partial z^2}+c_{14}\frac{\partial^2 v}{\partial x^2}-c_{14}\frac{\partial^2 v}{\partial y^2}+2c_{14}\frac{\partial^2 u}{\partial x\partial y}+(c_{44}+c_{13})\frac{\partial^2 u}{\partial x\partial z}+(c_{44}+c_{13})\frac{\partial^2 v}{\partial y\partial z}=\rho\frac{\partial^2 w}{\partial t^2}.
\end{aligned}
\tag{1}
$$

In the case of α quartz, the X and Z axes are chosen, respectively, as the digonal (electric) and trigonal (optic) axes. In the case of tourmaline the plane $x=0$ is chosen as a plane of symmetry and the Z axis is chosen as the axis of trigonal symmetry. This is the convention adopted by Voigt.

An inspection of the strain energy function written by Love[7] for the crystalline class to which quartz and tourmaline belong shows that this function leads to components of stress which differ from those given by Voigt.[8] In view of this situation, the reduction of the elastic constants for α quartz and tourmaline has been repeated by the writers. It was found that Voigt's reduction is correct and that the results summarized by Love are referred to a set of axes in which the choice of X and Y is the opposite of that described in the preceding paragraph. The choice of axes is not explicitly stated by Love but is incorrectly implied by him to be identical with that of Voigt.

The considerations which follow apply to free rectangular plates in which the origin of the Cartesian coordinates is located at the center of the parallelepiped. The x, y and z dimensions are respectively $2x'$, $2y'$ and $2z'$.

The boundary conditions are the statements that the boundaries of the parallelepiped are free from the normal components of surface traction. These statements, as they apply to this case, do not appear to have been summarized in the literature. Upon the notion of stress as described by Love,[9] these statements are as follows:

$$
\begin{aligned}
&X_x=0 \text{ when } x=\pm x'; \quad Y_z=0 \text{ when } y=\pm y',\ z=\pm z';\\
&Y_y=0 \text{ when } x=\pm y'; \quad Z_x=0 \text{ when } x=\pm x',\ z=\pm z';\\
&Z_z=0 \text{ when } z=\pm z'; \quad X_y=0 \text{ when } x=\pm x',\ y=\pm y'.
\end{aligned}
\tag{2}
$$

The Longitudinal Mode f_x

The terminology for the various crystal cuts is that described by Cady.[10] For example, an X cut is one whose major surfaces are normal to the X axis. It is implied that in this cut the x dimension $2x'$ is shorter than the y or z dimensions.

The frequencies of the longitudinal modes which are possible in the X, Y or Z cuts will be

[1] H. Osterberg, Proc. Nat. Acad. Sci. **15**, 892 (1929).
[2] H. Osterberg, J. Opt. Soc. Am. **22**, 19 (1932).
[3] H. Osterberg, J. Opt. Soc. Am. **23**, 34 (1933).
[4] H. Osterberg, Phys. Rev. **43**, 819 (1933).
[5] H. Osterberg, Rev. Sci. Inst. **5**, 183 (1934).
[6] Love, *The Mathematical Theory of Elasticity*, 1927, p. 83.
[7] Reference 6, p. 158.
[8] Voigt, *Lehrbuch der Kristallphysik*, 1910, p. 585.
[9] Reference 6, p. 73.
[10] W. G. Cady, Proc. I. R. E. **18**, 2136 (1930).

approximated with the assumption that the displacements are limited to the direction of propagation. (Such modes will be designated as pure longitudinal modes.)

Consider the mode in which compressional wave trains are propagated along X in an X, Y or Z cut. Under the above assumption $u=f_1(x, t)$ so that (1) reduces to

$$c_{11}\partial^2 u/\partial x^2=\rho\partial^2 u/\partial t^2. \quad (3)$$

When the differential equation is solved in the usual way, the frequency f_x of the longitudinal mode is found to be

$$f_x=(n/4x')(c_{11}/\rho)^{\frac{1}{2}}, \qquad n=1, 2, 3, \text{ etc.}, \quad (4)$$

in which n is the number of the harmonic.

The existence of this mode has been verified with the simple[11] and refracting[5] interferometers in both quartz and tourmaline plates of large x dimension. The characteristic positions of the antinodes of vibration of the X, Y and Z faces of a rectangular quartz plate are represented in Figs. 1 and 2 for the indicated harmonics by the shaded areas. These antinodes bear a definite orientation with respect to the crystallographic axes. When Figs. 1 and 2 are rotated through 180° about the X axis, the antinodes upon the opposite Y and Z faces occupy the same position with respect to the reader. This mode is easily excited by applying the electric field in any direction, through either full or strip electrodes placed upon the X, Y or Z faces. In quartz the X direction is preferred when it is desired to obtain the greatest amplitude of oscillation in the case of the odd harmonics for a given exciting voltage; in tourmaline, the Z direction.

It is instructive to decrease the x dimension of this Y cut resonator of Figs. 1 and 2, observing the effects produced upon the various harmonics. The number of harmonics which can be definitely recognized by the interferometer methods becomes smaller until only the first harmonic remains. As the x dimension is further reduced and the first harmonic observed, the X faces cease to vibrate with uniform amplitude. Simultaneously, the antinodes upon the Y and Z faces undergo changes as regards their relative amplitude, their form and position. The observed frequency departs from the computed frequency. With further reduction in the x dimension, the plate becomes a thick X cut, i.e., one in which the x dimension is appreciably smaller than the y or z dimensions. A group of patterns may now appear; but the presence of the fundamental in any one of these patterns can no longer be definitely recognized. On the other hand, no pattern may appear within a wide range of the computed value of f_x. The characteristics of the patterns in a thinner cut are without exception determined to such an extent by other modes of vibration that the influence or presence of the mode f_x is not to be detected.

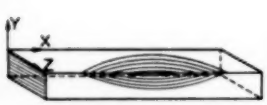

FIG. 1. First harmonic.

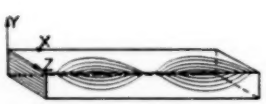

FIG. 2. Second harmonic.

It has been called to the writers' attention that in the ordinary X cut f_x should not be expected to be observed by interferometer methods since it is undoubtedly masked by flexural vibrations of greater amplitude. In this event, f_x should not be regarded as playing an important part in determining, for example, the practical usefulness of a given vibrational mode for frequency stabilization until it has been conclusively demonstrated to do so. The flexural vibrational patterns are, however, easily separated from the longitudinal patterns by means of the refracting interferometer.[5] In this instrument the flexural vibrations are not directly observed (except in very special cases) although they may be present together with longitudinal patterns which are simultaneously under observation. Although the refracting interferometer is a sensitive instrument for detecting f_x, with its aid conclusive evidence for the presence of f_x in thin X cuts has not thus far been obtained. For lack of a better word, the term "vibrational pattern" will henceforth be used to denote the actual arrangement of nodes and antinodes in any given resonance response of a vibrating plate. The term "mode" will be used to denote any one of the more specific arrangements of nodes and antinodes whose superposition and mechanical coupling determines the "vibrational pattern." The observations of the preceding paragraph should not be interpreted to mean

[11] H. Osterberg, J. Opt. Soc. Am. **23**, 34 (1933).

that the longitudinal mode f_x does not exist in a thin X cut. But these observations do emphasize that in thin X cuts, f_x is only of secondary importance in determining the various characteristics of the vibrational patterns.

The above observations are in disagreement with those in a recent paper by Bergmann[12] who lists the first sixty-nine harmonics of f_x in a moderately thick X cut. These harmonics were determined by an indirect method. Since quartz plates vibrate at an enormous number of frequencies, it is unreliable to determine the type of vibration either from the coincidence of the observed and computed frequencies or from indirect methods of observations. The conclusions of many investigators are open to this criticism.

Some of the crystals used in these experiments are described in Table I. These were carefully

TABLE I. *Crystals.*

CRYSTAL	MATERIAL	CUT	x(mm)	y(mm)	z(mm)
1	Quartz	Y	54.58	2.907	26.57
2	"	Y	35.141	3.535	74.35
3	"	Z	38.989	22.537	4.262
4	"	Y	70.541	10.739	30.919
5	"	Z	52.855	10.482	3.064
6	"	Y	51.486	2.972	4.089
7	"	Y	47.749	0.977	10.988
8	"	Y	54.58	2.907	7.184
9	"	Y	35.249	5.650	10.186
10	"	Y or Z	60.188	18.646	15.784
11	Tourmaline	Y or Z	11.001	3.312	3.139
12	Quartz	X	3.790	48.423	10.277
13	Tourmaline	X or Z	3.238	14.837	3.593
18	Quartz	Y	62.243	10.549	17.991
19	"	Y or Z	62.243	11.603	17.991
20	"	X, Y or Z	10.381	10.382	10.385

cut, ground and polished by the writers. They are rectangular within 1/100 degree. Their orientation with respect to the crystallographic axes is within one-fourth degree of that specified. The crystals were of optically flawless quartz.

Eq. (4) enables one to determine the elastic constant c_{11} from measurements upon f_x. The crystal plates were excited through electrodes which were coupled directly or inductively to a Hartley oscillator. The resonance frequencies were obtained by tuning the oscillator for maximum amplitude of oscillation of the crystal plate which was simultaneously observed in an appropriate interferometer. Experiments employing a beat method previously described[13] show that the frequency which corresponds to the maximum amplitude of oscillation is critical and can be consistently duplicated within ten cycles for a given input voltage to the Hartley oscillator. The dependence of this resonance frequency upon the input voltage and therefore upon the amplitude of vibration of the plate does not appear to have been recorded. As an example, the first harmonic of crystal 10 could be caused to resonate at frequencies extending from 44.99 to 45.18 kc/sec. This is a frequency difference of 0.44 percent. The highest resonance frequency is always associated with the lowest input voltage or the smallest amplitude of vibration. This dependence of frequency upon amplitude is observable in every mode of vibration and should be taken into account in selecting the resonance frequencies used in determining c_{11}. It is much less marked in the higher overtones. Tests show also that it is not entirely a matter of external damping introduced by the method of mounting. Whenever any marked difference occurred, the resonance frequency which corresponded to the lowest input voltage was selected.

TABLE II. c_{11} *in quartz.*

CRYSTAL	HARMONIC	f(kc/sec.)	V_x(cm/sec.) ($\times 10^5$)	c_{11}(dynes/cm^2) ($\times 10^{10}$)
1	2	98.00	5.349	77.21
"	3	151.3	5.505	80.43
"	4	200.4	5.469	79.38
"	5	251.3	5.486	79.87
"	6	299.3	5.445	78.69
"	7	350.0	5.458	79.06
"	8	400.5	5.465	79.26
"	9	450.5	5.464	79.24
"	10	499.5	5.458	79.06
"	11	551.8	5.476	79.59
"	12	599.8	5.456	79.00
"	13	649.0	5.450	78.83
"	16	797.3	5.440	78.54
2	1	77.65	5.457	79.03
"	2	155.8	5.475	79.55
"	3	232.3	5.442	78.60
"	4	310.0	5.447	78.74
3	1	69.37	5.409	77.65
"	2	142.5	5.556	81.93
"	3	210.3	5.466	78.71
"	4	297.7	5.452	78.89
"	5	349.0	5.443	78.63
4	1	38.72	5.463	79.21
"	3	116.14	5.462	79.18
5	1	51.45	5.430	78.25
"	2	102.1	5.397	77.31
"	3	153.7	5.416	77.85
6	2	105.1	5.412	77.74
"	3	157.7	5.412	77.74
"	4	210.1	5.406	77.56
"	5	263.7	5.431	78.29
7	1	56.77	5.421	77.99
"	2	114.9	5.486	79.87
"	3	170.5	5.427	78.17
8	1	100.1	5.463	79.21
9	1	77.15	5.439	78.51
"	2	154.6	5.449	78.80
			Average	78.79
			Giebe and Scheibe	78.43
			Voigt	85.14

[12] L. Bergmann, Hochfreq. Tech. u. Elek. **43**, 83 (1934).
[13] Osterberg and Cookson, Rev. Sci. Inst. **5**, 284 (1934).

TABLE III. c_{33} *in quartz and tourmaline.*

CRYSTAL	MATERIAL	x(mm)	y(mm)	z(mm)	Harmonic	V(cm/sec.)	c_{33}(dynes/cm^2)
						($\times 10^5$)	($\times 10^{10}$)
14	Quartz	19.848	2.907	18.395	1	6.309	105.6
					2	6.242	103.4
15	Quartz	35.141	16.068	74.350	3	6.220	102.7
						Average	103.8
						Voigt	105.4
16	Tourmaline			15.735	1	7.229	162.0
17	Tourmaline	5.345	4.507	14.803	1	7.342	167.1
					2	7.313	165.8
						Average for plate No. 17	166.5
						Voigt	160.4

The measurements of c_{11} are listed in Table II and compared with the value which has been averaged by the writers from the frequencies listed in Table III[14] of the publication by Giebe and Scheibe. A comparison is also made with the value of c_{11} determined by Voigt,[15] who employed a static method. His value is 7.7 percent higher and appears to be inconsistent with these data. It will be noted that the reciprocal of c_{11}, 1.28 $\times 10^{-12}$ cm^2/dyne, compares more favorably with the value of $s_{11}(1.27\times 10^{-12})$ determined by Voigt. Giebe and Scheibe used the frequency formula, $f_x=(n/4x')(s_{11}\rho)^{-\frac{1}{2}}$. This may be deduced upon the same assumption as that made in the derivation of Eq. (4). Within the validity of the assumption that the displacement u is due to a pure compressional wave propagated along X, it follows that $c_{11}=s_{11}^{-1}$. An examination of the relations which exist between the elastic constants c_{ij} and the elastic moduli s_{ij} shows that the latter equality is not, in general, true. This is but one of the many examples of the approximate nature and of the obvious inadequacies of the present day theories concerning vibrating elastic solids. One should not form the opinion that, on the other hand, the theories which concern the deformations of solids under static stress are fully adequate. More accurate theories for computing the frequencies of vibration of flexural and longitudinal modes in quartz plates have been formulated by the writers. These indicate that the above method is a reliable one for measuring c_{11} and that, for example, the value of c_{12} as determined by Voigt should be regarded only as of the right order of magnitude.

The list of frequencies in Table II represents a typical portion of the data collected for determining c_{11} from f_x. The frequencies of the vibrational patterns which were shown by interferometer methods to contain the mode f_x tightly coupled with some other mode are not listed in this table. The spread of the values of c_{11} was clearly shown by interferometer methods to be due mainly to mechanical coupling.

It is perhaps not trivial to remark that the "pure" compressional wave train which was considered in the brief derivation of (4) is essentially a plane wave train. There is nothing in this derivation which restricts the applicability of (4) either to thin or to long X cuts. In view of the approximate nature of the theory leading to (4), the applicability of this formula to any particular X cut should be based solely upon how well this formula fits the experimental facts. From this point of view and the observations of the preceding paragraphs the formula is inapplicable to the vibrational pattern of a thin X cut. The arguments[16, 17] from which it has been concluded that the formula should hold accurately in the limiting case in which y'/x' or z'/x' becomes infinite are not substantiated by the observations made with the interferometer.

c_{11} was measured in tourmaline from the first harmonic of crystal 11. This specimen was Brazilian tourmaline of light bluish tint. It was not optically uniform. The corresponding frequency, velocity and value of c_{11} are, respectively, 415.5 kc/sec., 9.142×10^5 cm/sec. and 259.1 $\times 10^{10}$ dynes/cm^2. Voigt's value of c_{11} is 4 percent higher. The density of crystal 11 was found to be 3.024 g/cc from a measurement of its weight. The value $\rho=3.100$ was used in computing c_{11}.

[14] Giebe and Scheibe, Ann. d. Physik (5) **9**, 93 (1931).
[15] Reference 8, p. 754.
[16] I. Koga, Physics **3**, 70 (1932).
[17] Mason, Bell Sys. Tech. J. **13**, 444 (1934).

FIG. 3. Motion of front surfaces.

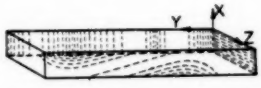

FIG. 4. Motion of back surfaces.

THE LONGITUDINAL MODE f_y

In pure compressional wave trains which are propagated along Y, $v=f_2(y, t)$ so that from (1)

$$c_{11}\partial^2 v/\partial y^2=\rho\partial^2 v/\partial t^2. \qquad (5)$$

The solution is similar to that of (3). One finds that

$$f_y=(n/4y')(c_{11}/\rho)^{\frac{1}{2}}, \qquad n=1, 2, 3, \text{ etc.} \qquad (6)$$

This mode has been found in quartz and tourmaline plates of long y dimension. The changes which occur in the harmonics of f_y upon shortening the y dimension are similar to those which occur in the harmonics of f_x upon shortening the x dimension. The mode cannot be recognized in the interference patterns of Y cuts of small y dimension. Recent observations made at this laboratory with the aid of the simple interferometer upon plates of quartz have shown that the actual manner of vibration of the mode whose frequency is approximated by (6) is more complicated than that described in Figs. 1 and 2. The characteristic positions of the antinodes of the first harmonic are represented by the shaded areas in Figs. 3 and 4. The Z faces vibrate with considerable amplitude. (The more heavily shaded areas indicate greater amplitude of vibration.) The pattern suggests that the wave fronts do not travel directly from one Y face to the other but are reflected also from the Z faces. The antinodes of the higher harmonics bear a similar orientation with respect to the plate. This pattern may prove to be so complicated that it cannot be properly classified as due to pure compressional waves which are propagated along Y. In this event, these experiments do not support the existence of the mode f_y.

The longitudinal modes f_z and f_y have not been studied thoroughly in tourmaline plates, but preliminary observations indicate that their displacements are similar to those of quartz plates.

A large number of suitable X cuts were not ground for measuring c_{11} from f_y, whose existence has just been questioned. A reliable measurement was secured for quartz from the first harmonic of crystal 12. The corresponding frequency, velocity and value of c_{11} are, respectively, 56.50 kc/sec., 5.471×10^5 cm/sec. and 79.44×10^{10} dynes/cm^2. As was also noted by Giebe and Scheibe,[18] the value of c_{11} measured from f_y is almost one percent higher than that measured from f_x. This difference arises, without a doubt, from the peculiar lateral vibrations of the mode f_y. For this reason the better value of c_{11} is that measured from f_x, i.e., 78.79×10^{10} dynes/cm^2.

c_{11} in tourmaline was measured from the first harmonic of the mode f_y in crystal 13 which was ground from Brazilian tourmaline, reddish in color and nonuniform in optical character. The frequency of the vibration and the corresponding value of c_{11} are, respectively, 305.0 kc/sec. and 254.0×10^{10} dynes/cm^2.

THE LONGITUDINAL MODE f_z

For the case in which pure compressional wave trains are propagated along Z, $w=f_3(z, t)$. From (1):

$$c_{33}\partial^2 w/\partial z^2=\rho\partial^2 w/\partial t^2. \qquad (7)$$

When sinusoidal solutions are chosen to satisfy the boundary condition $Z_z=0$, where $z=\pm z'$, one finds that

$$f_z=(n/4z')(c_{33}/\rho)^{\frac{1}{2}}, \qquad n=1, 2, 3, \text{ etc.} \qquad (8)$$

This mode was found in both quartz and tourmaline. From the observations that quartz plates of long z dimension usually exhibited patterns which corresponded to a few of the higher harmonics of f_z it appears that this mode can be excited in quartz plates only when it is mechanically coupled with other modes of vibration. In the case of the few excitable harmonics the crystal would respond no matter which electrode arrangement was used and no matter in which direction the electric field was applied.

On the other hand, the lower harmonics of this mode are easily excited in tourmaline plates of long z dimension. In exciting the odd harmonics in tourmaline, the electric field is most

[18] Giebe and Scheibe, Ann. d. Physik (5) **9**, 101, 103 (1931).

effectively applied when its direction is that of Z. The changes which occur in the harmonics as the z dimension is cut down are similar to those described in the case of f_x. Evidence for the existence of this mode in thin Z cuts of either quartz or tourmaline has not been secured. In this connection the measurements of G. W. Fox,[19] who employed plates of tourmaline, require discussion. The method employed by Fox involved the coincidence of the observed and computed frequencies as a criterion for determining the mode of vibration. Coincidence was secured by grinding the edges of the plates and their z dimensions. Two of these plates were kindly sent to the writers by G. W. Fox. One Z face of each plate was polished with slight reduction of the z dimension. When these plates were examined in the simple interferometer over a wide frequency range about the computed first harmonics, no vibrational patterns appeared in which f_z was definitely recognized. There were several active responses in the neighborhood of the computed frequency, but these were shown to be flexural in character.

The data for determining c_{33} in quartz and tourmaline are assembled in Table III. Crystals 16 and 17 were, respectively, of dark blue and light blue tint. They were optically inhomogeneous. The elastic constants of tourmaline appear to vary with the type of tourmaline. Voigt's determination of c_{33} is in better agreement both in quartz and in tourmaline with that of the vibratory method than is his determination of c_{11}.

The Simple and Pure Shear Modes

The terms shear, simple shear, pure shear and transverse have been applied so loosely to certain modes of vibration of quartz plates that it has become necessary to describe these terms. According to Love's definition of simple[20] and pure[21] shear, the displacements u, v and w are linear functions of the Cartesian coordinates. Modes of vibration which belong to the cases listed in the next paragraph and whose displacements are linear functions of the coordinates in accordance with the definitions of Love will be denoted as the simple shear or pure shear modes. A transverse mode is one in which the displacements produced by the standing wave trains are perpendicular to the directions of propagation of these trains. The term shear is here reserved for denoting those vibrational modes whose displacements may be described by means of the components of shearing strain e_{yz}, e_{zx} and e_{xy}. In any specific mode the term shear is qualified by an adjective indicating which one or which combination of these components of shear is involved.

The simple shear, pure shear and transverse modes are conveniently classified as follows: case A, $u=f_4(y, t)$; B, $u=f_5(z, t)$; C, $v=f_6(x, t)$; D, $v=f_7(z, t)$; E, $w=f_8(x, t)$; F, $w=f_9(y, t)$. In case A, Eq. (1) reduce to

$$[(c_{11}-c_{12})/2](\partial^2 u/\partial y^2)=\rho\partial^2 u/\partial t^2. \qquad (9)$$

This differential equation is not satisfied by periodic displacements of the form

$$u=aye^{i\omega t}, \qquad \omega\neq 0. \qquad (10)$$

Similarly, solutions do not exist for the simple shear modes B, C, D, E and F. More generally, Eqs. (1) are not satisfied by periodic displacements which are linear functions of x, y and z. Vibrational patterns corresponding to the simple shear modes were not found with the aid of the simple interferometer in a large variety of X, Y and Z cuts of quartz. The Y cut was examined the most carefully since the application of electric fields along Y introduces shearing forces[22] which tend to bring about shear displacements of the form $u=by$. These forced displacements assume the periodicity of the electric field. Their amplitudes are readily calculated by including the piezoelectric forces. But there are no observed resonance frequencies. Theory and experiment show that the simple and pure shear modes of free vibration do not exist.

The Transverse Modes

Eq. (9), case A is satisfied by transverse solutions of the form

$$u=a\cos\beta y\cdot e^{i\omega t} \quad \text{or} \quad b\sin\beta y\cdot e^{i\omega t}. \qquad (11)$$

[19] G. W. Fox and M. Underwood, Physics **4**, 10 (1933).
[20] Reference 6, p. 35.
[21] Reference 6, p. 33.
[22] W. G. Cady, Phys. Rev. **29**, 617 (1927).

When β and ω are chosen to satisfy the boundary condition $X_y=0$ where $y=\pm y'$, the corresponding frequency f_{xy} is given by

$$f_{xy}=(n/4y')((c_{11}-c_{12})/2\rho)^{\frac{1}{2}},\quad n=1,\ 2,\ 3,\ \text{etc.}\quad (12)$$

This mode has been designated by Koga[23] as the pure shear mode. His frequency is equal to $2f_{xy}$ but an examination of his derivation will show that f_{xy} should be obtained when the major surfaces are free. It was hoped to excite this mode in a Y cut by applying the electric field along Y and to observe the vibrational pattern by forming interference fringes between an X face and an auxiliary plate of glass. Evidence for the existence of this mode was not found even when high exciting potentials (perhaps 10,000 volts) were applied to crystals 1, 10, 18, 19 and 20. The mode was similarly sought without success in a number of thin Y cuts of the type used by Koga and Lack-Willard-Fair.[24]

In a recent report by Straubel[25] the interferometer patterns of Figs. 2 and 3 are said to illustrate the "nebenschwingungen" or the vibrations which may accompany the supposed shear mode in special Y cuts. It is not clear whether the term shear is applied to the simple shear, the pure shear or the transverse mode. The pattern of Fig. 3 is simpler than that of Fig. 2 and is of a type which has been frequently observed by the writers. In this pattern the eighth flexural overtone in which flexural waves are propagated along the length of the plate appears to be mechanically coupled with the ninth overtone in which flexural waves of greater amplitude are propagated along the width of the plate. Now, in vibrational patterns in which flexural wave trains are propagated along X in a Y cut the motions of the X faces are similar to those in the fundamental of the theoretical mode f_{xy}. These two modes are easily differentiated by examining the corresponding motions of the Y faces. When these modes resonate at the same frequency, their separation should theoretically be effected by reducing the y dimension since this reduction decreases the frequency of the flexural mode and increases the frequency of the transverse mode. Since this reduction of the y dimension does not appear to have been carried out by Straubel, his interference patterns are not accepted by the writers as evidence either for or against the existence of the theoretical mode f_{xy}.

According to Straubel, Bechmann[26] and Lack-Willard-Fair, the temperature coefficient of the transverse mode is zero in suitably oriented Y cuts. We seriously question this conclusion until the transverse mode has been shown to exist. It may be that these low temperature coefficients are associated with flexural modes of vibration. They are being measured at this laboratory by a method which permits the vibrational pattern of the heated crystal to be observed with the aid of interference fringes. The coefficients are small between 20 and 100°C. They may be positive or negative. Beyond 300°C they are definitely negative until the transition point is reached. The interference patterns show that crystals of β-quartz continue to oscillate even at 800°C. The temperature coefficients are positive in β-quartz. It will be shown elsewhere that β-quartz is actually piezoelectric.

The wave equations which correspond to the transverse cases B, C, D, E and F are, respectively,

$$c_{44}\partial^2u/\partial z^2=\rho\partial^2u/\partial t^2,\quad (13)$$

$$[(c_{11}-c_{12})/2]\partial^2v/\partial x^2=\rho\partial^2v/\partial t^2,\quad (14)$$

$$c_{44}\partial^2v/\partial z^2=\rho\partial^2v/\partial t^2,\quad (15)$$

$$c_{44}\partial^2w/\partial x^2=\rho\partial^2w/\partial t^2,\quad (16)$$

and

$$c_{44}\partial^2w/\partial y^2=\rho\partial^2w/\partial t^2.\quad (17)$$

The corresponding modes of vibration have been sought in a number of suitable crystals without success with the aid of the simple interferometer. The electric fields were applied along X, Y and Z through both full and strip electrodes.

It is concluded from these observations upon the transverse modes A–F that these modes, if they exist at all, are of only secondary importance in determining the vibrational patterns of quartz plates of the usual orientation.

[23] I. Koga, Reports of Radio Research and Works in Japan **2**, 157 (1932).
[24] Lack, Willard and Fair, Bell Sys. Tech. J. **13**, 453 (1934).
[25] H. Straubel, Physik. Zeits. **35**, 179 (1934).
[26] R. Bechmann, Naturwiss. **21**, 752 (1933).

The yz Shear Mode

According to Mason,[27] rectangular plates of α quartz may enjoy a mode of vibration whose displacements are described with good approximation by the shear component e_{yz}. This mode is here denoted as the "yz shear mode." In the case of a free plate the frequency expression has been shown by Mason to be

$$f_{np}=(1/4)(c_{44}/\rho)^{\frac{1}{2}}(n^2/y'^2+p^2/z'^2)^{\frac{1}{2}}. \quad (18)$$

This frequency relation and the expressions for the displacements v and w are here briefly derived since we believe that the boundary conditions have not been properly satisfied by Mason.[27]

Mason's wave equation, (30), p. 447 may be written

$$\begin{aligned}\rho\partial^2 v/\partial t^2&=c_{44}(\partial^2 v/\partial z^2+\partial^2 w/\partial y\partial z),\\ \rho\partial^2 w/\partial t^2&=c_{44}(\partial^2 w/\partial y^2+\partial^2 v/\partial y\partial z).\end{aligned} \quad (19)$$

One finds that solutions of the type

$$\begin{aligned}v&=B\cos\beta y\sin\gamma z\cos\omega t,\\ w&=R\sin\beta y\cos\gamma z\cos\omega t\end{aligned} \quad (20a)$$

or

$$\begin{aligned}v&=B\sin\beta y\cos\gamma z\cos\omega t,\\ w&=R\cos\beta y\sin\gamma z\cos\omega t\end{aligned} \quad (20b)$$

satisfy (19) provided

$$\begin{aligned}c_{44}\gamma/B(B\gamma+R\beta)-\rho\omega^2&=0,\\ c_{44}\beta/R(B\gamma+R\beta)-\rho\omega^2&=0.\end{aligned} \quad (21)$$

Consequently

$$R=\beta B/\gamma \quad \text{and} \quad c_{44}(\beta^2+\gamma^2)-\rho\omega^2=0. \quad (22)$$

The boundary conditions (2) may be derived from and are equivalent to Mason's Eqs. (28). It is not possible to choose β and γ so as to satisfy every requirement of (2). Thus, if in the case of (20a) $\cos\gamma z'=\cos\beta y'=0$, $Y_z=0$ when $y=\pm y'$ and $Z_z\neq 0$ when $z=\pm z'$. If one chooses $\sin\gamma z'=\sin\beta y'=0$, $Y_z\neq 0$. It is also found that this dilemma is not avoided by considering the more general displacements

$$\begin{aligned}v&=\sum\sum B_{mn}\cos\beta_m y\sin\gamma_n z\cos\omega t\\ w&=\sum\sum R_{mn}\sin\beta_m y\cos\gamma_n z\cos\omega t.\end{aligned} \quad (23)$$

[27] Mason, Bell Sys. Tech. J. **13**, 430, 446 (1934).

In solutions of the type (20a or b) it is not possible to choose β and γ such that the surfaces of the vibrating plate shall be free of every normal component of surface traction. The writers are unable to exhibit any other type or combination of other types of solutions which will completely satisfy both (1) and (19).

Solutions (20a or b) can however be made to satisfy the following boundary conditions: It will be noted that for these solutions $e_{yy}(=\partial v/\partial y)$ and $e_{zz}(=\partial w/\partial z)$ are in general different from zero. These solutions involve therefore both extensions and shear. Suppose that prior to the instant $t=0$ the rectangular plate is subjected to the static stresses $X_x=Y_y=Z_z=Z_x=X_y=0$ and $Y_z=Q$. The new boundary conditions are the statements that the surface tractions shall assume the above values at $t=0$, $x=\pm x'$, $y=\pm y'$, and $z=\pm z'$. These require that in the case of (20a)

$$\cos\beta y'=\pm\cos\gamma z'=\pm 1 \quad (24)$$

and determine both B and R in terms of Q since (22) must still hold. In the case of (20b)

$$\sin\beta y'=\pm\sin\gamma z'=\pm 1 \quad (25)$$

and both B and R are determined in terms of Q. Similar comments apply to the more general type of solutions (23). When the values of β and γ which are consistent with (24) and (25) are substituted into (22), this expression becomes identical to (18) in which $n=1, 2, 3$, etc., and $p=1, 2, 3$, etc. The choice of (20a or b) is not arbitrary but depends upon the values of the integers n and p.

A careful study of this derivation will show that the choice of neither $n=0$ nor $p=0$ is allowed.

Vibrational patterns in which the presence of the yz shear mode could be definitely recognized have not been found with the aid of the interferometers in rectangular plates of α quartz of the usual orientation with respect to the crystallographic axes. The presence of this mode has, however, been recognized in the vibrational patterns studied with the aid of the interferometers in the case of rectangular plates oriented after the manner described by Mason and by Lack, Willard and Fair. Eqs. (20a and b) and

(18) are inadequate in describing the displacements and frequencies of these vibrational patterns. The yz shear mode is only of secondary importance in determining these characteristics of any of the observed vibrational patterns. None of the observed vibrational patterns even approximately obey (20a and b) and (18).

The xy Shear Mode

The term "xy shear mode" is used to denote the mode of vibration whose displacements are chiefly determined by the strain component e_{xy}. When certain "coupling elasticities" are neglected after the manner followed by Mason[28] in the case of the yz shear mode, one obtains the wave equations:

$$\rho\partial^2 u/\partial t^2 = c_{66}(\partial^2 u/\partial y^2 + \partial^2 v/\partial x\partial y),$$
$$\rho\partial^2 v/\partial t^2 = c_{66}(\partial^2 v/\partial x^2 + \partial^2 u/\partial x\partial y). \tag{26}$$

When solutions of the type

$$u = A \cos \alpha x \sin \beta y \cos \omega t,$$
$$v = B \sin \alpha x \cos \beta y \cos \omega t \tag{27}$$

are substituted into (26) and made to satisfy the boundary conditions $X_x = Y_y = Z_z = Y_z = Z_x = 0$ and $X_y = P$ at $t = 0$, $x = \pm x'$, $y = \pm y'$ and $z = \pm z'$, the frequency f_{mn} of vibration is found to be

$$f_{mn} = (1/4)(c_{66}/\rho)^{\frac{1}{2}}(m^2/x'^2 + n^2/y'^2)^{\frac{1}{2}}, \tag{28}$$

$m = 1, 2, 3$, etc., $n = 1, 2, 3$, etc.

The presence of the xy shear mode in the vibrational patterns of X, Y or Z cuts of the usual orientation in α quartz has not been clearly recognized by means of the interferometers. However, this mode has been found by the interferometer methods in Y cuts of the special orientations described by Lack, Willard and Fair. When the angle θ[29] of orientation is suitable, Eqs. (27) and (28) describe the corresponding displacements and frequencies with a *fair* degree of accuracy. The most suitable angles of orientation have not yet been determined. The amplitude of oscillation in the case of $f_{mn} = f_{11}$ may easily reach two wavelengths of light (5461A) even with low exciting voltages (less than 250 volts) in the case of crystal plates whose x, y and z dimensions are as small as or greater than 0.75 cm.

To understand the following brief comments, the reader should study the papers written by Mason[27] and Lack, Willard and Fair.[24] In specially oriented Y cuts c_{66} must be replaced by its value in the new orientation, namely, c_{66}'. (For brevity in the exposition, the priming of Y, Z and y in the specially oriented cuts is here omitted.) The wave equation, (26), can be derived accurately only when $c_{56}' = 0$. Otherwise, one is forced to neglect the terms which contain c_{56}'. There are two angles θ for which $c_{56}' = 0$. These are the most suitable angles mentioned in the preceding paragraph. So far, the data which have been secured at this laboratory indicate that the convention which has been adopted by Mason with regard to when θ shall be taken as positive or negative is in error. The angles for which $c_{56}' = 0$ will be determined and reported elsewhere together with a new set of values for the elastic constants of α quartz.

The failure of (20a and b) and (18) to describe the vibrational patterns containing the yz shear mode is to be expected. It is not possible to orient a plate of α quartz in such a manner that all of the "coupling elasticities" which have been neglected in the derivation of (19) can be reduced to zero.

The choice of either $m = 0$ or $n = 0$ is inconsistent with the theory leading to (28). In case it were possible to choose $m = 0$,

$$f_{0n} = (n/4y')(c_{66}'/\rho)^{\frac{1}{2}}, \tag{29}$$
$$u = A \sin n\pi y/2y' \cos \omega t, \quad n = 1, 3, 5, \text{ etc.},$$
$$u = A \cos n\pi y/2y' \cos \omega t, \quad n = 2, 4, 6, \text{ etc.}$$

If the forbidden transverse mode (29) can be regarded as a special case of the xy shear mode, one may conclude from purely theoretical reasons that the transverse mode (12) cannot exist. Similarly, one could also show that the remaining transverse modes belonging to cases A to F of a preceding section do not exist. It has already been stated that the interferometer data have presented no evidence for the existence of any one of the transverse modes. In view of these data and the theories of this and preceding

[28] Reference 27, p. 447.
[29] Reference 27, p. 450.

sections, the writers conclude that the mode of vibration employed by Lack, Willard and Fair was not a transverse mode of vibration. This is contrary to their conclusion.

The following considerations may explain some of the parasitic frequencies observed by Lack, Willard and Fair and indicate that the mode employed by them was the xy shear mode. The ratio of the y dimension to the x or z dimensions in the plates described by them is of the order of 1/20. When x' is replaced by $20y'$ in (28)

$$f_{mn}=(1/4y')(c_{66}'/\rho)^{\frac{1}{2}}(m^2/400+n^2)^{\frac{1}{2}}. \quad (30)$$

The various frequencies in the series f_{11}, f_{21}, f_{31}, etc., differ only slightly in magnitude, particularly for small values of m. When full electrodes are used, only those harmonics can theoretically be excited in which both m and n are odd. This decreases the number of extra harmonics, or parasitic responses which occur in the neighborhood of f_{11}, but these parasitic frequencies become numerous in thin Y cuts. In any harmonic f_{m1} there appear two antinodes upon the X faces and $m+1$ antinodes upon the Y faces. These antinodes of displacement bear a strong resemblance to those of the $m-2$ harmonic of the flexural mode, in which the standing flexural wave train is propagated along the X axis. These two modes are distinguishable by the simple expedient of reducing the y dimension since this reduction increases the frequency of the xy shear mode and decreases the frequency of the flexural harmonics.

The zx Shear Mode

Except for the comments on the Y cuts employed by Lack, Willard and Fair, whatever has been said about the xy shear mode in the preceding section applies also to the zx shear mode provided v is replaced by w, y by z and n by p. The interference data indicate that the xy and zx shear modes are inextricably bound together except for those angles θ for which $c_{56}'=0$. The values of the elastic constants determined by Voigt do not appear to be reliable enough for calculating this angle. Both the xy and zx shear modes are easily excited in properly oriented cuts by applying the electric field (through full or partial electrodes) in the Y direction.

The writers wish to express their gratitude to Professor J. R. Roebuck for his helpful cooperation in these problems and for his criticisms of the manuscript. We are indebted also to the National Research Council for grants toward purchasing the raw quartz and tourmaline used in these experiments.

Erratum: The Flexure Problem for Rectangular Beams with Slits

Dwight F. Gunder, *University of Wisconsin and Colorado State College*

(Physics **6**, 38, 1935)

USING the term two-beam action in the sense explained by Newlin, Heck and March,[1] *viz.*, that the shearing stress in the neutral plane is relieved as a consequence of the partially independent action of the upper and lower halves of the beam, the last sentence of the paper should be modified to state that two-beam action occurs in the case of both shallow and deep checks. According to the above interpretation the effect of two-beam action was found in wooden beams with both moderate and deep checks.

[1] Newlin, Heck and March, Trans. A.S.M.E. **56**, 739 (1934).

Notice to Contributors

Manuscripts

Send manuscripts to John T. Tate, University of Minnesota, Minneapolis, Minnesota.

Papers must be in English, typewritten double spaced with wide margins.

Abstracts

An abstract must accompany each article. It should be adequate as an *index* and as a *summary*. As an index it should give all subjects, major and minor, concerning which new information is presented. As a summary it should give the conclusions of the article and all numerical results of general interest.

References

References should appear as footnotes, numbered consecutively, and arranged thus:

A. B. Smith, Phys. Rev. **41**, 852 (1932).

Captions and Legends

Legends for figures must accompany manuscript. Each table should have a caption. These in all cases should be complete in themselves so as to make the data intelligible to the reader without reference to the text.

Mathematical Expressions

Make all expressions clear to the typesetter. Identify in the margin of the manuscript Greek letters and unusual symbols.

Use fractional exponents instead of root signs.

Avoid complicated exponents and subscripts. Should it be necessary to repeat a complicated expression a number of times it should be represented by some convenient symbol.

The solidus (/) should be used wherever possible for fractions.

Illustrations

Plan figures for approximately one-half reduction. Wherever possible arrange figures so that after reduction they will not be wider than three inches. Lettering must be large enough to be readable after reduction.

Line drawings must be made with India ink on white paper or tracing cloth. Coordinate paper is not desirable, but if used must be blue-lined and all coordinates to be reproduced drawn with India ink.

Drawings which cannot be used will be returned to the author or redrawn at his expense.

Photographs should show clear black and white contrasts.

Avoid round and oval photographs.

Publication Charge

A portion of the cost of publishing the results of research must be regarded as an integral part of the cost of the research. In keeping with the policy which is effective for the Institute's publications a bill for $3.00 per page will be sent to the authors of papers appearing in this journal. It is intended that the authors shall present these bills for payment to the institutions which have supported their researches. If the institution is unable to make payment the bills are to be returned marked "No Funds Available."

Reprints

As a partial return for the publication charge one hundred reprints without covers will be furnished free. Additional reprints may be obtained at a regular schedule of prices.

Alterations

Take great care that each manuscript is typographically accurate. A limited number of alterations in proof are unavoidable, but the cost of making extensive alterations after the article has been set in type will be charged to the author.

Proof and all correspondence concerning papers in the process of publication should be addressed to the Editorial Secretary, American Institute of Physics, 11 East 38th Street, New York, N. Y.

THE AMERICAN PHYSICAL SOCIETY

R. W. WOOD, *President*
The Johns Hopkins University
Baltimore, Maryland

F. K. RICHTMYER, *Vice President*
Cornell University
Ithaca, New York

W. L. SEVERINGHAUS, *Secretary*
Columbia University
New York, New York

G. B. PEGRAM, *Treasurer*
Columbia University
New York, New York

JOHN T. TATE, *Editor*
University of Minnesota
Minneapolis, Minnesota

L. B. LOEB, *Local Secretary for the Pacific Coast*
University of California
Berkeley, California

THE object of the American Physical Society is the advancement and diffusion of the knowledge of physics. It sponsors *The Physical Review*, *Physics* and the *Reviews of Modern Physics*. Upon the recommendation of two or more members, any person engaged in work in the field of physics or actively interested in physics may become a member; receive one of the journals; receive also *Science Abstracts* A, *The Review of Scientific Instruments with Physics News and Views*, and the Bulletin of all meetings; and attend and participate in the seven annual meetings.

Annual dues: $10. Fellows, $14.

For further information address the Secretary as above.

THE SOCIETY OF RHEOLOGY

S. E. SHEPPARD, *President*
Eastman Kodak Company
Rochester, New York

EUGENE C. BINGHAM, *Editor*
Lafayette College
Easton, Pennsylvania

A. STUART HUNTER, *Secretary & Treasurer*
Du Pont Rayon Company
Buffalo, New York

THE Society of Rheology was formed in 1929 to advance the science of the deformation and flow of matter. It cooperates with the American Physical Society in editing *Physics* of which four issues per year are devoted to *Rheology*. All persons interested are invited to become members and participate in the proceedings at the annual December meetings. Members receive without other charge than their dues all issues of *Physics*, *The Review of Scientific Instruments with Physics News and Views* and the notices of the Society.

Annual dues: $6.

For further information address the Secretary as above.